ARMY RESEARCH LABORATORY

Development of a Multistream Acoustic Propagation Model Including Scattering by Turbulence

By Harry J. Auvermann
Battlefield Environment Directorate

Richard L. Reynolds
University of Texas at El Paso

Daniel M. Brown
Scientex of Texas

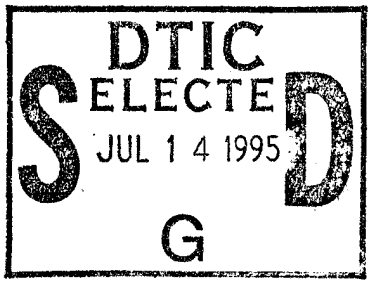

ARL-TR-528 June 1995

NOTICES

Disclaimers

The findings in this report are not to be construed as an official Department of the Army position, unless so designated by other authorized documents.

The citation of trade names and names of manufacturers in this report is not to be construed as official Government indorsement or approval of commercial products or services referenced herein.

Destruction Notice

When this document is no longer needed, destroy it by any method that will prevent disclosure of its contents or reconstruction of the document.

REPORT DOCUMENTATION PAGE

Form Approved
OMB No. 0704-0188

1. AGENCY USE ONLY (Leave blank)	2. REPORT DATE	3. REPORT TYPE AND DATES COVERED
	June 1995	Final

4. TITLE AND SUBTITLE

Development of a Multistream Acoustic Propagation Model Including Scattering by Turbulence

5. FUNDING NUMBERS

6. AUTHOR(S)

Harry J. Auvermann, Richard L. Reynolds, and Daniel M. Brown

7. PERFORMING ORGANIZATION NAME(S) AND ADDRESS(ES)

U.S. Army Research Laboratory
Battlefield Environment Directorate
ATTN: AMSRL-BE-S
White Sands Missile Range, NM 88002-5501

8. PERFORMING ORGANIZATION REPORT NUMBER

ARL-TR-528

9. SPONSORING / MONITORING AGENCY NAME(S) AND ADDRESS(ES)

U.S. Army Research Laboratory
2800 Powder Mill Road
Adelphi, MD 20783-1145

10. SPONSORING / MONITORING AGENCY REPORT NUMBER

ARL-TR-528

11. SUPPLEMENTARY NOTES

12a. DISTRIBUTION / AVAILABILITY STATEMENT

Approved for public release; distribution is unlimited.

12b. DISTRIBUTION CODE

A

13. ABSTRACT *(Maximum 200 words)*

The objective of the ARL research effort in acoustic propagation is to provide the Army with a multistream model for investigating acoustic detection systems operating in a variety of realistic battlefield conditions. The first step is to account for scattering from turbulent regions of the atmosphere with an explicit algorithm. The turbulent region is considered to be a collection of vortices with a distribution of characteristic sizes and velocities and random orientation and position. Each vortex (turbule) is characterized as a known (or assumed) velocity distribution in three dimensional space. The scattering from each turbule is determined by solving the fluid equations. The contribution to the sound pressure level at the detector location of all turbules is summed up accounting for the propagation characteristics of the atmospheric medium. The algorithms devised to model the above picture of the turbulent region are then used in existing (or appropriately modified) propagation models. Progress in incorporating turbulence scattering into the Fast Field Program (FFP) acoustic propagation model is recounted in this report.

14. SUBJECT TERMS

acoustic propagation, multistream, turbulence scattering

15. NUMBER OF PAGES

89

16. PRICE CODE

17. SECURITY CLASSIFICATION OF REPORT	18. SECURITY CLASSIFICATION OF THIS PAGE	19. SECURITY CLASSIFICATION OF ABSTRACT	20. LIMITATION OF ABSTRACT
Unclassified	Unclassified	Unclassified	SAR

Acknowledgment

The authors would like to acknowledge the assistance of Dr. John Noble of ARL in carrying out the work here reported. Dr. Noble supplied the version of FFP used and assisted our learning to use the code. He also supplied the codes that, with the addition of range/elevation loops and input/output statements, became the codes named Spherical and Limitray used below.

Contents

Figures

Appendix Figures

Appendix Tables

1. Introduction

Acoustic propagation in the atmosphere is influenced by a number of factors that have to be considered in any model designed to predict detector response at battlefield distances. The accompanying figure 1 illustrates a possible scenario that incorporates most of the factors of interest. The figure also shows the importance of acoustics as a non-line-of-sight detection tool for the Army. In the figure, an object of interest, marked S, is a source of acoustic field marked F. An acoustic detector, marked D, is some distance from the source. An obstruction, marked O and illustrated as a ridge, intervenes between S and D. This obstruction scatters F by diffraction into a secondary field marked E . Atmospheric turbulence, marked T, scatters F into another secondary field marked M. The ground surface itself, marked P, reflects F into a third secondary field marked R. The electronic signal from the acoustic detector D, marked V, is produced by a superposition of the direct field F (if any) with E, M, and R plus the intrinsic detector noise denoted by N.

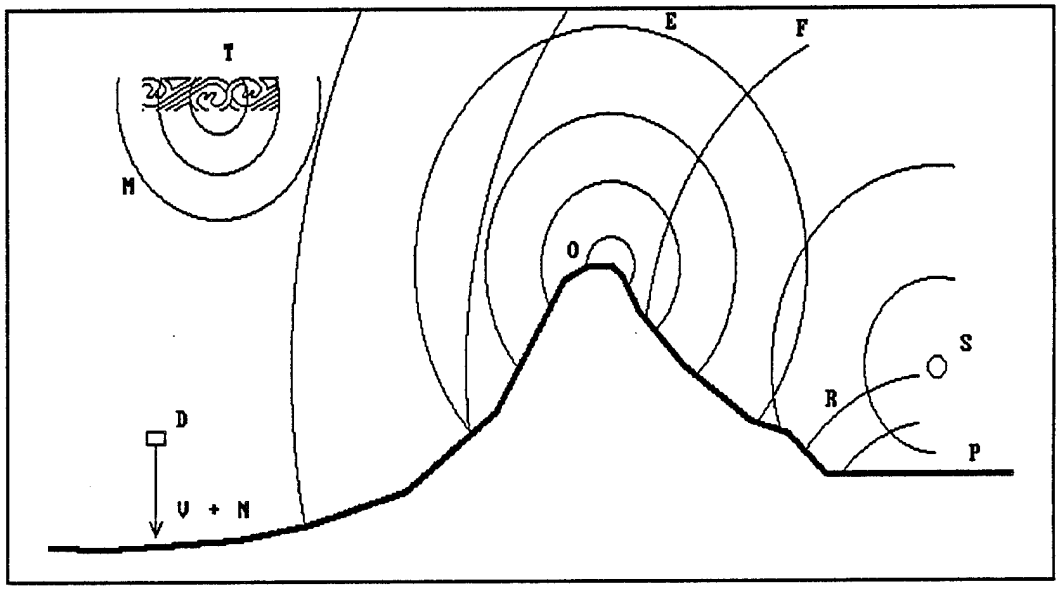

Figure 1. Acoustic detection scenario.

The problem of interest is to determine theoretically the detector signal V, and hence, the signal-to-noise ratio (SNR) (V/N)**2 given the scenario and the source characteristics.

A number of computer codes have been or are being developed to solve the problem posed in figure 1. The following is a list of some of them:

- Fast Field Program (FFP) - a two dimensional wave code that models a stratified atmosphere
- Parabolic Equation (PE) - a two dimensional wave code with additional features but very computationally intensive
- Infrasound - a two dimensional long range ray trace model from Los Alamos National Laboratory
- Sysnoise - three dimensional proprietary code of Dynamic Engineering
- 3D FFP - being worked on at Salford University in Great Britain
- 3D PE - reportedly being worked on in France
- Split Step PE - Army Research Laboratory's (ARL) Battlefield Environment Directorate (BED) has received a copy of this code recently
- FFP in C - ARL's BED has received a copy of this code recently
- Two-way Wave Equation - being worked on at Delft University, Netherlands

The context of the effort reported here is the desire for an advanced acoustic propagation model that can be used by the Army in the future. The ever lengthening distances over which the Army must operate will eventually require models that consider earth curvature. The wave codes listed above model a flat earth. Since the wave equation is formally the same for acoustic propagation as for electromagnetic propagation, a note about the latter is instructive. A solution to the global propagation of electromagnetic radiation from lightning was available in the 1950's, but the references have not been located. The reason global propagation is being looked into is the possibility that a new approach for the future acoustic propagation model such as that used in the 1950's electromagnetic code will be called for to account for earth curvature. This new approach would pare down from a global scale to the more modest battlefield scale.

In the short term, a starting point for the development of the future acoustic propagation model can be chosen for shorter distances wherein the flat earth assumption does not introduce unacceptable errors. Because it has the

capability of calculating sound propagation in a refractive atmosphere, accounts for ground reflection using a complex impedance formalism, and is computationally fast, the FFP code was chosen as the starting point for development. The approach is to add one feature at a time, starting with turbulence scattering.

This report describes the progress that has been made in modeling turbulence effects using FFP. Section 2 contains a description of a simplified scenario that is used in the remaining sections of the report. Section 2 also contains certain acoustic propagation calculations, using simplified theory which serve as orientation concerning the acoustic field levels to be expected. Section 3 describes how FFP has been augmented to account for multistreams. An acoustic field for an upward refracting atmosphere showing a shadow zone is compared with the simplified theory field of section 2. Section 4 treats turbulence scattering. Scattering cross section results for a single turbule are presented followed by theory and a sample calculation for incoherent summation of scattering from many turbules. Superposition of the direct and scattered fields completes section 4. Section 5 summarizes the findings of this work.

2. Acoustic Propagation on the Battlefield

The scenario of figure 1 is too complex for contemporary analytical techniques. In this section, a simplified scenario is defined and field calculations are made for a uniform atmosphere.

2.1 Simplified Scenario for this Report

For the purpose of this report, a more modest scenario is used rather than that of figure 1. This more modest scenario is illustrated in figure 2.

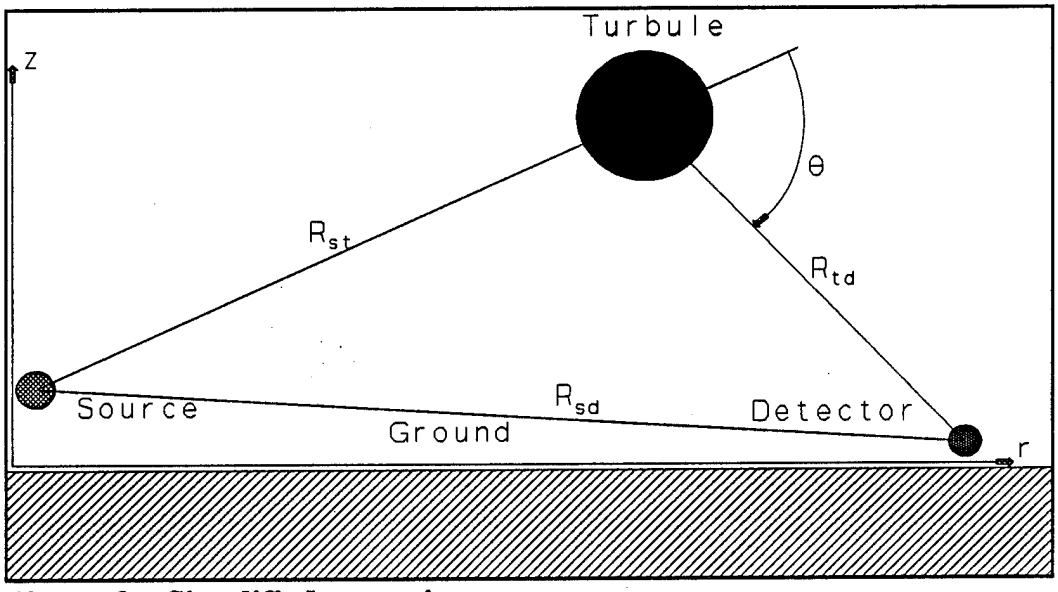

Figure 2. Simplified scenario.

Shown in figure 2 are a source, a detector, and a turbule positioned over flat ground. The coordinate system used is also shown. The horizontal coordinate variable is r, and z is the vertical coordinate variable. The scattering angle variable θ is also shown. The quantities R_{st}, R_{td}, and R_{sd} are slant range variables that are used in the calculations. The coordinates of the principal objects chosen for this scenario are as follows:

$$r_s = 0.0 \text{ m}, \quad z_s = 10.0 \text{ m}$$
$$r_t = 5000.0 \text{ m}, \quad z_t = 424.0 \text{ m}$$
$$r_d = 6000.0 \text{ m}, \quad z_d = 4.0 \text{ m}$$

Subscripts s, t, and d stand for source, turbule, and detector, respectively. With this geometric arrangement the scattering angle $\theta = .48$ rad, an angle that gives maximum scattering for the largest turbule accommodated by the turbule cross section theory discussed in section 4. The ranges were chosen to be representative of current battlefield distances used in modeling. The three slant distances are

$$R_{st} = 5{,}017.110 \text{ m}$$
$$R_{td} = 1{,}084.620 \text{ m}$$
$$R_{sd} = 6{,}000.003 \text{ m}$$

The symbol E is used for field exitance values with units $w \cdot m^{-2}$. The assumed value for this quantity at a distance of 1 m from the source is $E_s = 1.0\ w \cdot m^{-2}$.

Assuming an isotropic source (radiation the same in all directions) in an infinite uniform medium, the exitances at the turbule and at the detector are $E_{It} = 3.9728 \cdot 10^{-8}\ w \cdot m^{-2}$ and $E_{Id} = 2.7777 \cdot 10^{-8}\ w \cdot m^{-2}$, respectively.

For convenience, the logarithmic equivalents of these quantities in terms of decibels, called level, will be used for calculating excess attenuation. These are $L_{It} = 10 \log_{10}(E_{It}/E_s)$ db and $L_{Id} = 10 \log_{10}(E_{Id}/E_s)$ db.

The letter I in the above subscripts indicates these quantities are infinite space values.

2.2 Acoustic Propagation in a Uniform Atmosphere

As a check on the more sophisticated models, a propagation model called Spherical was written, which models a uniform atmosphere situated above a flat earth, the latter modeled by an impedance change. Spherical is described more fully in appendix B. Some results from this program are shown here. In figure 3 below, a contour plot from Spherical is shown, which represents the sound field for a uniform atmosphere, frequency of 170 Hz, source height of 10.0 m, sound speed of 340 m/s, and a ground porosity parameter of 134.0. The program calculated the ground impedance ratio to be 8.44 + j10.0 for this

porosity (see appendix B). The heavy line is the limit ray position calculated from the Limitray program. In an upward refracting atmosphere with a uniform sound speed gradient, the ray path is a circle. The limit ray is the circular path through the source location and tangent to the ground surface. For more information on this latter program, see appendix C. Figure 4 shows the region near the origin in greater detail with the horizontal and vertical scales the same. The interference between the direct and the ground reflected waves is clearly demonstrated. The contour plots in this report were done using the Mathematica software package. [1] The method employed to produce these plots is described in appendix D.

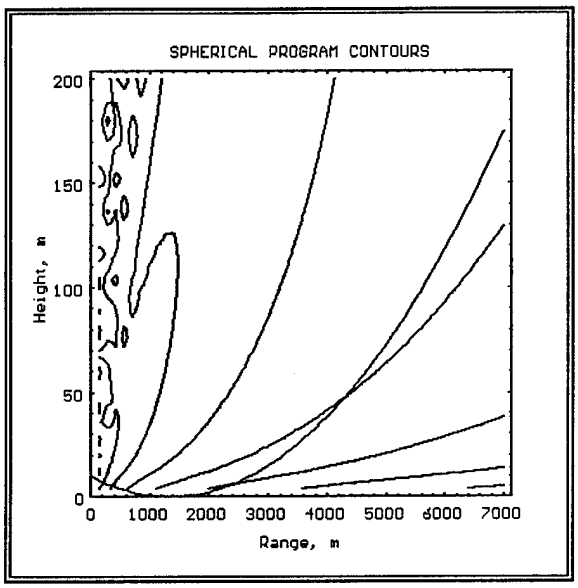

Figure 3. Spherical program contours for a uniform atmosphere (contour interval −10 db, eight contours starting at −40 db).

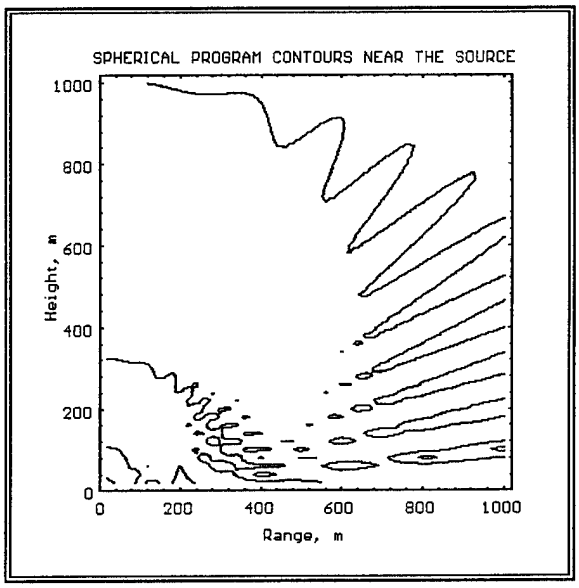

Figure 4. Spherical program contours near the source for a uniform atmosphere (contour interval −10 db, four contours starting at −30 db).

3. Multistream Acoustical Propagation

This section describes the FFP acoustic propagation model and how FFP was augmented to form the Acoustic Multistream Propagation Program (AMPP). The latter is able to calculate multistream effects such as turbulence scattering. AMPP is then exercised to compute the acoustic field in an upward refracting atmosphere. The latter is the simplest atmospheric circumstance that produces a shadow zone. This capability of AMPP to represent a shadow zone is a necessary ingredient in the demonstration of section 4 where scattering into a shadow zone is calculated.

3.1 FFP Acoustic Propagation Model

The FFP acoustic propagation model is a widely used code that has been developed over the years by the acoustics community. [2] Some background and characteristics of FFP are contained in the consultant's report. [3] FFP is two dimensional in that it considers only a vertical plane, such as that of figure 2. The ground is treated as a flat surface for which the ratio of ground impedance to atmospheric impedance at ground level may be specified. The atmosphere is treated as a layered medium with layer boundaries parallel to the ground. The atmospheric parameters are uniform within each layer. If the number of layers in the atmosphere is large, the task of preparing the input file is oppressive. This function has been automated in the program called MENU3. See appendix A for further information on MENU3. FFP is considered a single stream model in that it treats only a single outgoing wave. Future use by the Army for scenarios such as that shown in figure 1 require that multiple paths for the wave to reach the detector be considered. Development of such a multistream model is described in the next subsection, based upon the scheme devised by the consultant. [3] The final summation subroutine from this report, Xstrasc, has been included essentially unaltered. The tasks performed in the other subroutine from the report, Scatr, have been incorporated into the main routine AMPP. The angular scattering pattern function, Phi(theta), from the Born approximation mentioned in the documentation of Scatr has been set to unity here because FFP assumes isotropic sources.

3.2 AMPP

The AMPP calculates the sound pressure level at a detector that is subject to the field produced by a number of sources and a number of scatterers. Scatterers are considered isotropic sources whose amplitude and phase result from that produced at the scatterer location by some true source. The sound pressure wave produced by a scatterer is also proportional to a scattering cross section, which is an input quantity. The starting point in the development of AMPP is the FFP. FFP processes one acoustical source and one acoustical detector, producing several files as output. Those files represent the wave number, level, clip factor, and pressure of the sound at a set of ranges. The modules FFP calls are Input, Profil, Wavnum, Cutoff, Voltge, Smooth, and Four1, in that order. Other modules exist but are subordinate to the above modules. AMPP contains FFP as a subroutine. The remaining parts of AMPP carry out looping through the several sources and several scatterers preserving the resulting files for each iteration. Finally, AMPP appropriately sums the results for selected detector locations.

Figure 5 illustrates a block diagram of AMPP. The usual version of FFP consists of all subroutines inside the dashed lines in figure 5, plus the subroutine Input which would be immediately to the left of Profil. To convert FFP into a subroutine, the major modifications were as follows:

1. The call to subroutine Input was removed. Subroutine Input read in all variables for the program. Since some of the variables (i.e., source and detector) would change, the call to subroutine Input was moved to the main routine of AMPP.

2. The variables initialized by subroutine Input were passed to subroutine FFP as arguments or in common statements.

AMPP has its own unique Input subroutine, as seen in figure 5. The input variables of FFP are all present in the new Input subroutine, but others have been added. They include the phase of the source in relation to the other sources, and the ability to input up to 50 sources and 50 detectors. Once all input has been read into the program, AMPP iteratively calls subroutine FFP

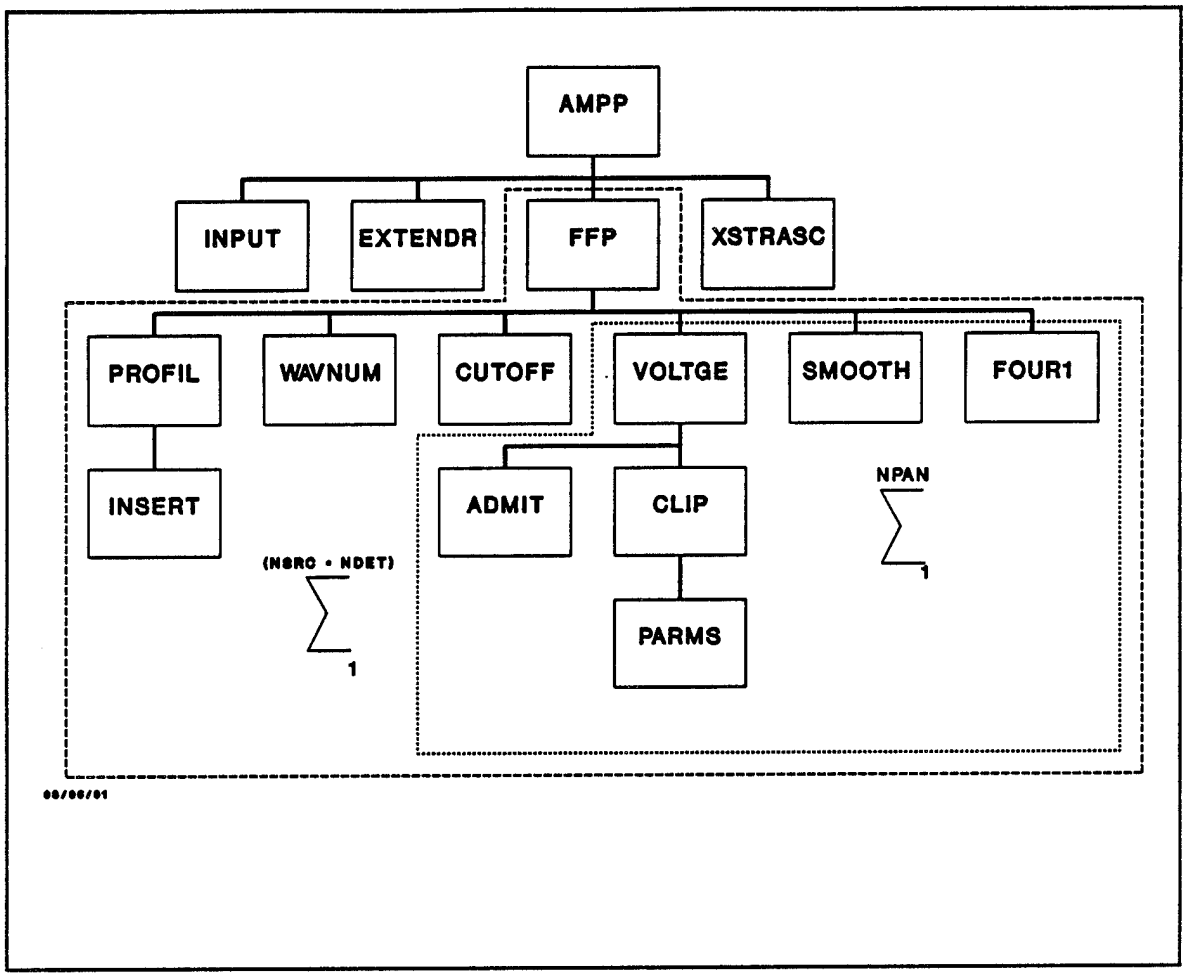

Figure 5. AMPP block diagram.

passing a single source and detector pair. If S is the number of sources, and D is the number of detectors, then FFP is called S*D times. Each call to subroutine FFP produces the normal output as mentioned above.

The problem of overwriting successive output was skirted by creating unique output filenames. An additional subroutine was written that took as input the source and detector numbers currently being processed, 1 through 50 for both source and detector. The subroutine Extendr returned a character string consisting of a two digit number representing the source, followed by a period, and finally a two digit number representing the detector. This was all appended to the original filenames, thus, creating a unique set of filenames for each iteration of subroutine FFP. As an example, the original name for the

wave number output file was WAVNUM.O. That same file for source 11 and detector 22, would become WAVNUM.O11.22.

Scatterers are both a source and a detector. A scatterer is represented by a source and detector that have the exact same height and range. In that instance, subroutine FFP will not be called using that source and detector number pair. Instead, the scatterers' amplitude and cross section are adjusted later in the Xstrasc subroutine. Subroutine Xstrasc was added to AMPP to combine all sources, coherent and incoherent, producing a comprehensive summation of what each detector would sense.

3.3 Acoustic Propagation in an Upward Refracting Atmosphere

To exercise the AMPP program, the scenario of figure 2 was calculated for an upward refracting atmosphere. The uniform sound speed gradient was $-3.7 \cdot 10^{-3}\ s^{-1}$ with speed at zero height of 335.1 m/s and a ground impedance ratio of 8.44 − j10.0. A different sign convention in FFP from that in Spherical requires a sign change in the imaginary part of the ground impedance. The heavy line in each figure is the limit ray path from program Limitray. As seen by comparison of figure 6 with figure 3, Spherical and AMPP show virtually identical contours out to a range of 1000 m. Beyond 1000 m, the AMPP −80 db contour parallels the limit ray path to a high degree of accuracy. The plot in figure 7 shows in greater detail the sound pressure level in the shadow zone below the limit ray path for the range interval 5000 to 7000 m. Inspection of figure 3 shows that interference between direct and reflected waves produces low sound pressure levels in this region even with a uniform atmosphere (i.e., with no shadow zone).

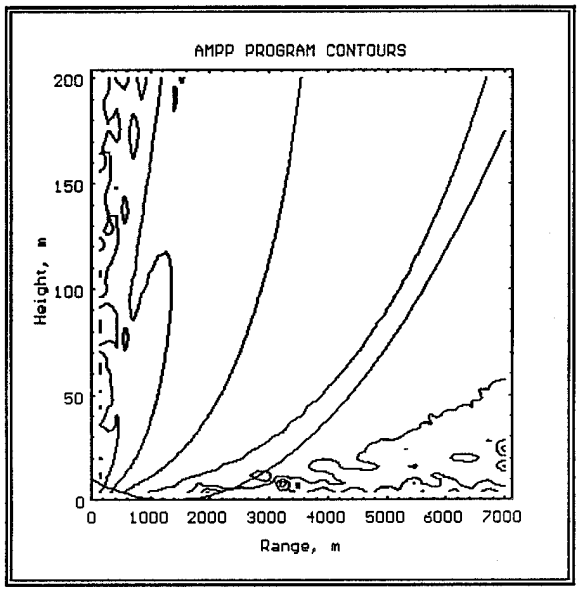

Figure 6. AMPP program full range results for an upward refracting atmosphere (contour interval −10 db, eight contours starting at −40 db).

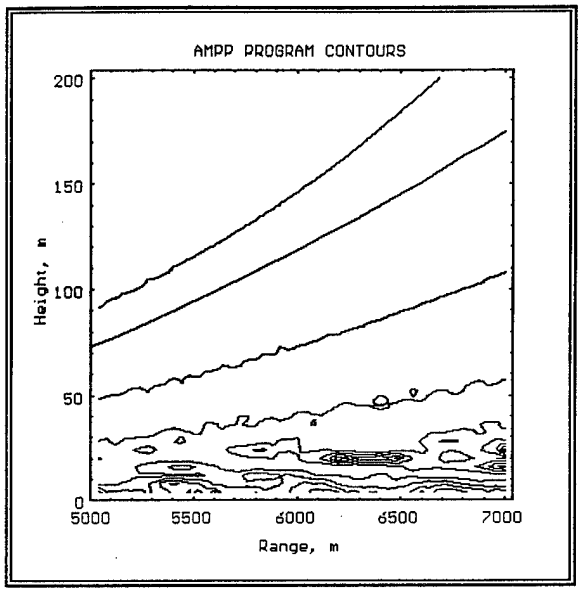

Figure 7. AMPP program results for an upward refracting atmosphere (contour interval −5 db, eight contours starting at −80 db).

4. Acoustic Scattering from Turbulence

In this section, a theory of scattering from a single turbule is summarized. Then this theory is used to determine the scattering from a collection of turbules in infinite, but otherwise uniform, space. Finally, these results are used with the results from AMPP calculations to show superposition of the direct field and the scattered field.

4.1 Explicit Acoustic Scattering from Turbules

To model turbulence scattering as scattering from a collection of turbules, it is necessary to have a means of calculating the scattering efficiency of each turbule. A Short Term Analytical Services (STAS) effort was initiated with Dr. George H. Goedecke, Department of Physics, New Mexico State University, to determine the acoustic scattering properties of moving density inhomogeneities. A report that contains results summarized below is available. [4]

Theory is developed for acoustical scattering by localized quasistatic atmospheric turbulent structures (turbules) that contain both flow and density variations. The quasistatic density variation is shown to be proportional to v^2, where v is the (presumably small) ratio of flow speed to asymptotic acoustical wavespeed. The flow contributes terms $O(v^2)$ to the scattering cross sections, while the density variations contribute terms $O(v^4)$. Differential and total cross sections have been calculated for a Gaussian spinning turbule model of effective radius a, for size parameters ka from 0.25 to 2.0, where $k = 2\pi/\lambda$, λ = wavelength. These calculations used the first Born approximation, which is estimated to be valid for $ka < 2$ for $v_{max} < 0.1$. The contributions of the density variation are about three orders of magnitude smaller than those of the flow. The latter are proportional to $(ka)^6$ and the product $[\sin(\theta)\cos(\theta)\cos(\theta_\alpha)\sin(\phi - \phi_\alpha)]^2$, where (θ,ϕ) are the (polar, azimuthal) scattering angles and $(\theta_\alpha,\phi_\alpha)$ are the spin axis angles. The contributions of the density variations vary as $(ka)^4$ and have a somewhat Rayleigh-like dependence on θ.

Figures 8, 9, and 10 from Goedecke [4] show the characteristics of turbule scattering to first order in v. Analytical results (appendix B) from this theory for turbule scattering efficiency averaged over turbule spin axis orientation are used in section 4.2 below. [4] These results are summarized here.

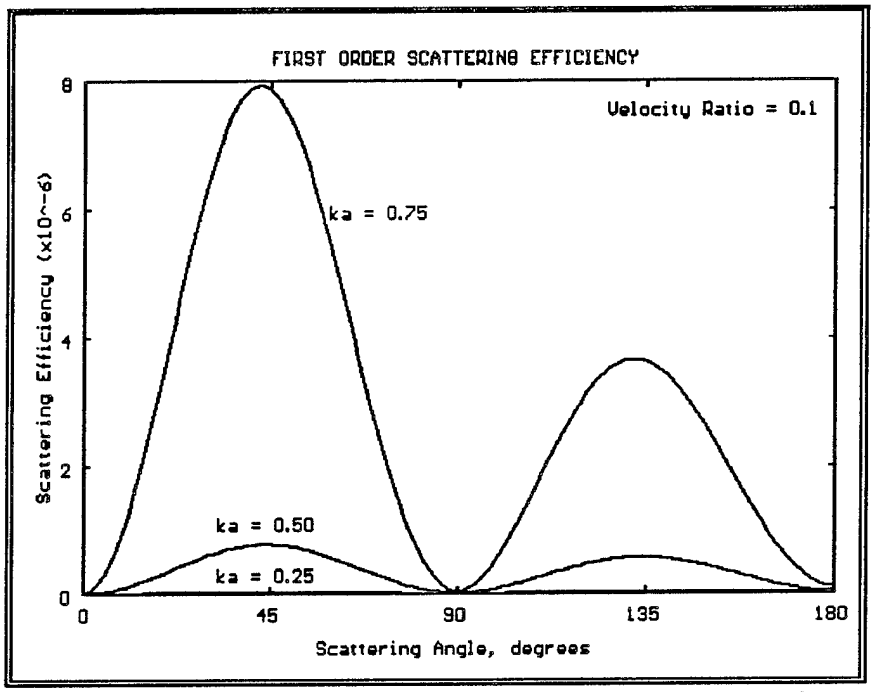

Figure 8. Average differential scattering efficiency for a small spinning turbule.

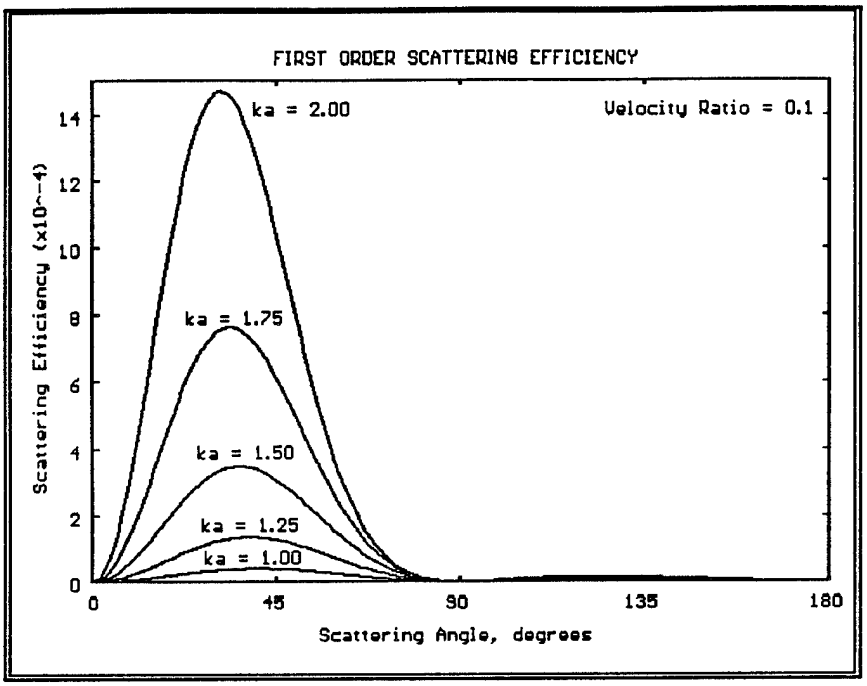

Figure 9. Average differential scattering efficiency for a spinning turbule.

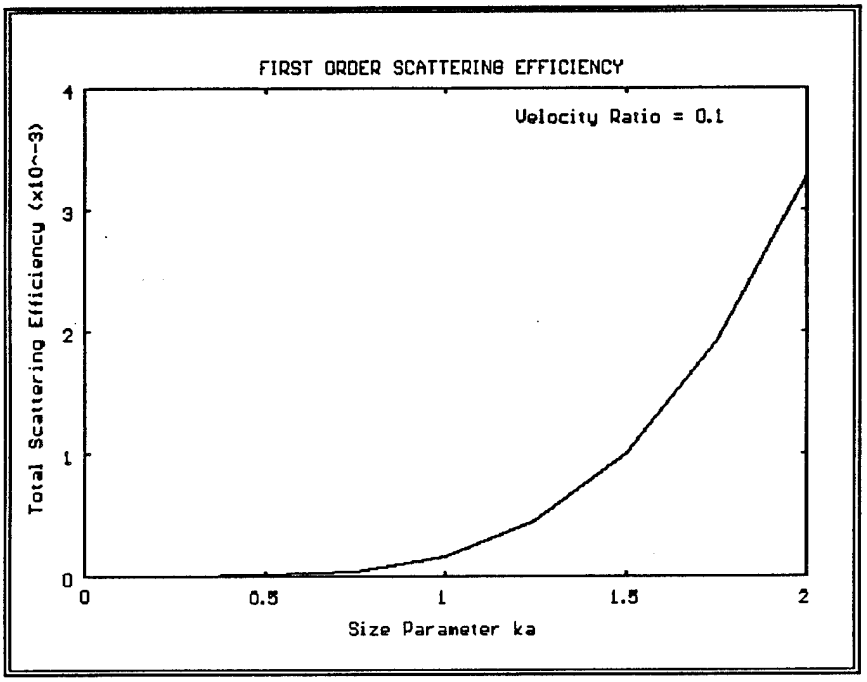

Figure 10. Total average scattering efficiency for a spinning turbule.

The following (quasi) static flow velocity $\vec{v}(\vec{r})$ and molecular number density $n_0(\vec{r})$ were chosen for a representative spinning turbule:

$$\vec{v}\ (\vec{r}) = (\vec{\Omega}\times\vec{r})\ \exp\ (-r^2/a^2) \tag{1}$$

$$n_0\ (\vec{r}) = -n_\infty v^2/(2c_\infty^2). \tag{2}$$

This represents a non-uniformly spinning turbule, with angular velocity parameter Ω about an axis $\hat{\Omega}$ through the origin of coordinates. The quantities (n_∞ and c_∞) are the background (number density and wavespeed) far from the turbule; the parameter a is an effective radius of the turbule; $\vec{r}$ is the position vector. The expression for $n_0(\vec{r})$ follows approximately from the assumption that turbules are formed adiabatically.

If an acoustic plane wave with propagation vector $\vec{k}$, where $k = 2\pi/\lambda = \omega/c_\infty$, ω = angular frequency, is incident upon this representative turbule, then the scattering amplitude $f(\vec{k},\hat{r})$ in the first Born approximation is given by

$$f\ (\vec{k},\hat{r}) = f^{(1)} + f_n^{(2)} + f_v^{(2)}, \tag{3}$$

where $f^{(1)}$ is linear in Ω, and $f^{(2)}$ is quadratic in Ω. The subscript n identifies the part of the scattering amplitude associated with number density variation and the subscript v identifies the part of the scattering amplitude associated with flow. The differential scattering cross section then turns out to be given by

$$\sigma(\vec{k},\hat{r}) = |f^{(1)}|^2 + |f_n^{(2)} + f_v^{(2)}|^2 \equiv \sigma^{(1)} + \sigma^{(2)}. \tag{4}$$

The differential scattering efficiency first order in Ω , which is defined to be the scattering cross section $\sigma^{(1)}$ divided by the physical cross section πa^2, averaged over all spin axis orientations is

$$\langle Q^{(1)}\ (k,\hat{f})\rangle = \left(\frac{1}{3}\right)\left(\frac{\Omega a}{4c_\infty}\right)^2 (ka)^6\ (\sin\theta\cos\theta)^2\ \exp\ [-(ka)^2\ (1-\cos\theta)] \tag{5}$$

where

θ = the polar angle, the angle between the direction of propagation and the direction from the scatterer to the observation point.

If E_i is the incident exitance ($w \cdot m^{-2}$) of the sound field and $I(\theta)$ is the intensity ($w \cdot sr^{-1}$) of the remote scattered field at the off-axis angle θ, then

$$I(\theta) = \pi a^2 \langle Q^{(1)}\ (k,\hat{f})\rangle E_i. \tag{6}$$

The total scattering efficiency is

$$\langle Q^{(1)}(k)\rangle = \int d\Omega \langle Q^{(1)}\ (k,\hat{f})\rangle \tag{7}$$

where

$d\Omega$ = $\sin\theta\ d\ \theta d\ \phi$ = solid angle element

The analytic total scattering efficiency for $\sigma^{(1)}$ is

$$\langle Q^{(1)}(k)\rangle = (\pi/45)\ (\Omega a/c_\infty)^2 (ka)^6. \tag{8}$$

Some authors, especially in radar scattering, relate the differential scattering cross section to the ideal isotropic scatterer. The scattered field intensity from the ideal isotropic scatterer is the same for all scattering angles θ with magnitude of the total cross section times the incident exitance divided by 4π.

The actual field from a nonisotropic scatterer is then the magnitude of the previous sentence times an appropriate function of θ called the phase function. This information is provided to alert the reader that there is a quantity of 4π applied in the radar scattering concept that is not needed in the development of this report.

4.2 Turbulence Scattering in an Infinite Space

This section contains a rough draft calculation of the turbulence scattered acoustic exitance ($w \cdot m^{-2}$) to be expected using the research results available at the time of writing (10 Aug 91) and assumed values for other quantities needed. This calculation is included not as a representative value for use in system calculations, but rather an order-of-magnitude value to be used in further research.

The symbols used in the calculation are defined as follows:

$\langle Q^{(1)}(k,\hat{r})\rangle$	=	differential scattering efficiency
$\sigma_{sca}(a,v,\theta)$	=	single turbule differential scattering cross section, m^2
a	=	turbule characteristic size, m
v	=	turbule characteristic velocity, $m \cdot s^{-1}$
Ω	=	turbule angular velocity = v/a, s^{-1}
λ	=	acoustic wavelength, m
x	=	size parameter = $2\pi a/\lambda$
c_∞	=	asymptotic acoustic wave velocity = 340 $m \cdot s^{-1}$
θ	=	propagation direction to detector angle, rad
E_s	=	exitance of source at a distance of 1.0 m
E_t	=	exitance at center of turbulent scattering volume
E_d	=	exitance at detector
Ω_d	=	solid angle field of detector, sr
V_{sca}	=	scattering volume, m^3
n	=	turbule concentration (turbules per unit volume), m^{-3}
R_{st}	=	source to turbulence range, m
R_{td}	=	turbulence to detector range, m
R_{sd}	=	source to detector range, m
l	=	length of scattering volume, m

r_v = radius of scattering volume (assumed cylindrical), m
ϕ = detector field half-angle, rad

The geometry of the calculation is that of section 2 above. The following values have been assumed to give a consistent parameter set:

Ω_d = 1.0 sr
n = $(1/10)^3$ m^{-3}
l = 1000 m
λ = 2 m
a_0 = 1000 m
v_0 = 3 $m \cdot s^{-1}$

In the above, a_0, v_0 are the characteristic size and velocity of the largest turbule that is relevant for the geometry. The value of a_0 was selected as representative of a typical boundary layer thickness and v_0 was selected as representative of a typical wind velocity. In this type of calculation, it is necessary to restrict the volume of the atmosphere from which scattered energy is accepted by the detector, the scattering volume V_{sca}. We have chosen to do this by defining the detector field of view, Ω_d, and the length, l, and assuming the volume is cylindrical. The largest size parameter x_{max} that can be used reliably in the Born approximation is $x_{max} = 5.0$. [4]

Using the definition of the size parameter and x_{max}, the turbule size limit for the Born approximation is $a = 5/\pi$ m.

Assuming the turbule is spherical, the above concentration and size means that the turbule occupies a fraction (1/59.2) of space. The seeming arbitrary choice of parameters listed above, instead of being arbitrary, collaborate to produce this fraction thereby assuring no turbule overlap within a size class. To estimate the turbule velocity, use the velocity-size relationship $v^3 = C\,a$ from statistical turbulence theory where the constant C is v_0^3/a_0 or 0.027. Solving for v, we have $v = 0.3503$ $m \cdot s^{-1}$. [5]

Using the relation $\Omega_d = 2\,\pi(1 - \cos\phi)$, the detector field half-angle for the chosen scattering volume is $\phi = 0.5719 = 32.7°$.

The scattering volume radius is then $r_v = r_{td} \sin \phi = 587.1$ m.

From section 2, we have

$$R_{st} = 5{,}017.110 \text{ m}$$
$$R_{td} = 1{,}084.620 \text{ m}$$
$$R_{st} = 6{,}000.003 \text{ m}$$
$$E_{It} = 3.9728 \cdot 10^{-8} \text{ w} \cdot \text{m}^{-2}$$
$$E_{Id} = 2.7777 \cdot 10^{-8} \text{ w} \cdot \text{m}^{-2}.$$

The remaining calculations can now be made.

$$V_{sca} = \pi r_v^2 l = 1.083 \cdot 10^9 \text{ m}^3$$

$$\langle Q^{(1)}(k,\hat{r}) \rangle = 3.416 \cdot 10^{-4}$$

$$\sigma_{sca}(a,v,\theta) = 2.7181 \cdot 10^{-3} \text{ m}^2$$

$$E_t = E_{It} = 3.9728 \cdot 10^{-8} \text{ w} \cdot \text{m}^{-2}$$

$$E_d = E_t \, n \, V_{sca} \, \sigma_{sca}(a,v,\theta)/(R_{td})^2 = 2.5018 \cdot 10^{-3} \, E_t$$

$$= 9.9392 \cdot 10^{-11} \, E_s$$

$$L_{Id} = -75.563 \text{ db (from section 2)}$$

$$L_{td} = -100.026 \text{ db (from } E_d \text{ expression above).}$$

With this choice of parameters, the excess attenuation ($L_{Id} - L_{td}$) is 24.463 db. The evidence shows that the excess attenuation is somewhere between 20 and 30 db. [6] Taking a median value of 25 db, the calculated excess attenuation value is approximately correct. The data in the reference is for a frequency of several hundred hertz, whereas the above is for 170 Hz. In these analyses, the limit of the usefulness of the cross section results has been reached at the size parameter of 5.0. To go to higher frequencies would

require cross section for size parameters in excess of 25.0, which our Born approximation cross sections will not support.

The ratio of cell dimension (the side of a cube whose volume is that of the reciprocal of the concentration) to turbule diameter ($n^{-(1/3)}/(2\ a)$ is 3.14, which is probably large enough to prevent turbule interaction. Our parameter assumptions and scattering calculation algorithm (not considering the spectrum of turbule sizes, for example) are not precise enough at this time to warrant any definite conclusion about the reasonableness of the number concentration. The separation to diameter ratio 3.14 figure seems to be of the correct order of magnitude so that we can demonstrate superposition of fields using n as we do in the next section. The adjusted excess attenuation and level is $E_{tdadj} = 2.6309 \cdot 10^{-3}\ E_t$ (using n_{adj}) and $L_{tdadj} = 10\ \log_{10}(E_{tdadj}/E_s) = -2.5799$, respectively.

The primary purpose of this section is to show that the approach that considers turbulence consisting of a collection of turbules has the potential for explaining the unexpectedly high sound levels in shadow zones. Before this potential is realized, it will be necessary to determine a relative number concentration spectrum (variation of concentration with turbule size) that will match known turbulence characteristics. [5] Also, an absolute number concentration will be required, which will be appropriate for some postulated turbulence intensity value. Both of these problems are currently being worked on, but the answers are not yet available. In the absence of more reliable information, the quantity in $E_{tdadj} = 2.6309 \cdot 10^{-3}\ E_t$ and $L_{tdadj} = 10\ \log_{10}(E_{tdadj}/E_s) = -2.5799$ will be used as explained in section 4.3.

4.3 Turbulence Scattering into a Shadow Zone

AMPP treats a scatterer as an isotropic source, as all sources modeled by FFP are isotropic. The scattering pattern of turbules from section 4, figures 8 and 9, are not isotropic. Nevertheless, this isotropic approximation was included into AMPP to begin getting a feel for how the scattered field would superimpose upon the direct field. The scattered field is shown in figures 11 and 12 below for two scatterer positions at 5000-m range. The scatterer of figure 11 is at the location defined for figure 2 in section 2. The turbule field

in figure 12 is scattered from a height of 746.5 m. In figures 11 and 12, the heavy line indicates the limit ray path defining a boundary between the propagation zone and the shadow zone for the source at zero range and 10.0-m height. Interference between the reflected and direct scattered field is apparent in these figures. The contours in both are separated −5 db and there are three contours starting at −75 db. The contour levels in the figures do not represent the true scattered signal including the source-to-scatterer loss.

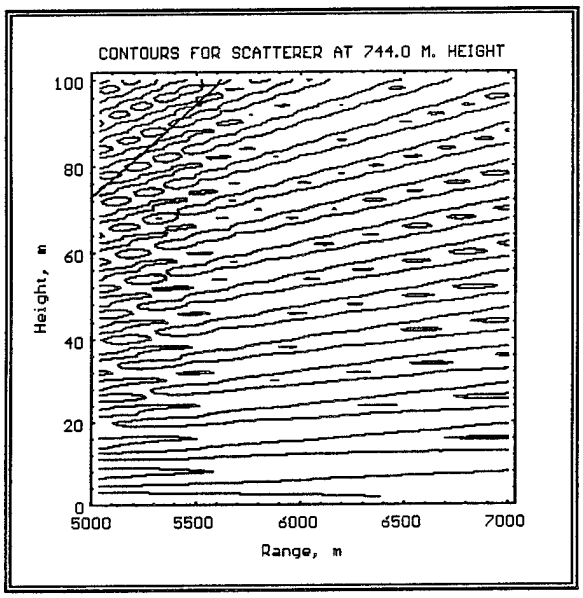

Figure 11. Turbule scattered field for scatterer height of 744.0 m.

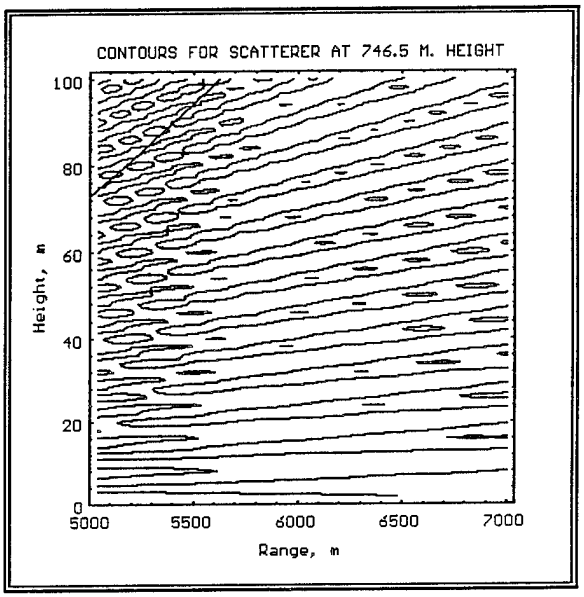

Figure 12. Turbule scattered field for scatterer height of 746.5 m.

Rather, they represent the signal as though the level at one meter from the scatterer was 1.0 $w \cdot m^{-2}$.

The calculation and discussion of section 6 above disclose the limitations that exist presently in the knowledge necessary for properly determining turbule scattering. The discussion below discloses the limitations present in shadow zone level calculations. Shadow zone levels as determined by AMPP are not low enough to allow display of scattered signals from small turbules that represent the present state of turbule cross section knowledge available. [4] The frequency is 170.0 Hz and the sound speed at ground level is 335.1 m/s so the wavelength is 1.97 m. The sound speed at the layer beginning at 733.3-m height is 332.4 m/s so the wavelength is 1.95 m, not a great deal different than that at ground level. Thus, the turbule field in figure 12 is

a height 1.276 wavelengths above that of figure 11. This height was chosen for display to show a definite difference in phase of the scattered wave. However, the interference pattern is apparently controlled by the distance from the reflecting boundary and not the source position because the two patterns are very similar. This situation is illustrated further in figure 13. This figure shows a vertical profile of the field at a range of 6000.0 m.

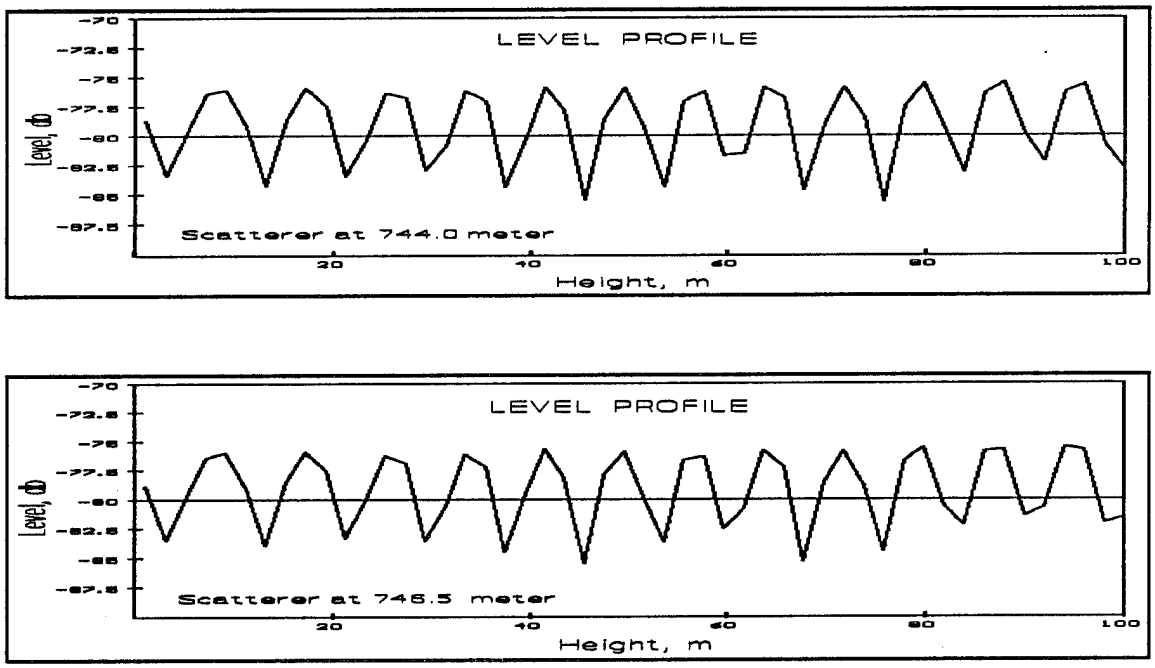

Figure 13. Vertical profiles of scattered fields at 6000 m.

The upper graph is for the scatterer at 744.0-m height and the lower graph is for the scatterer at 746.5-m height. Nevertheless, the summation at ground level, which has not been done here, will have to take into account the time difference of the two signals that are about $\pi/2$ rad out of phase.

The next exercise is to combine the direct field, that is shown in figure 6 with the scattered field, that is shown in figure 11. To see the scattered field, it is necessary to create an idealized primary field which is shown in figure 14. The data for figure 14 was generated from that for figure 6 by replacing all levels with a functional dependance. Above the -90 db contour, the levels were derived from circles with center coordinates (x and y) and radii are a

function of level. Below the −90 db contour the levels were derived from a cosine dependence on height. This cosine function was parameterized so that at 7000-m range the level and slope matched the function above −90 db. Also, the level fell to −150 db at 7000-m range and zero height. The cosine function was slid along the −90 db contour to calculate the levels between 5000- and 7000-m range. The contours of figure 11 modified by the scattering power loss of equation (3) are shown in figure 15.

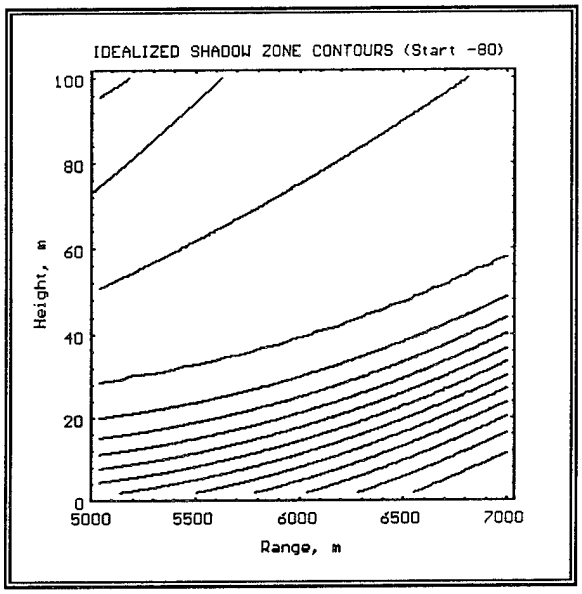

Figure 14. Idealized shadow zone contours (contours at −80 to −145 in 5-db intervals).

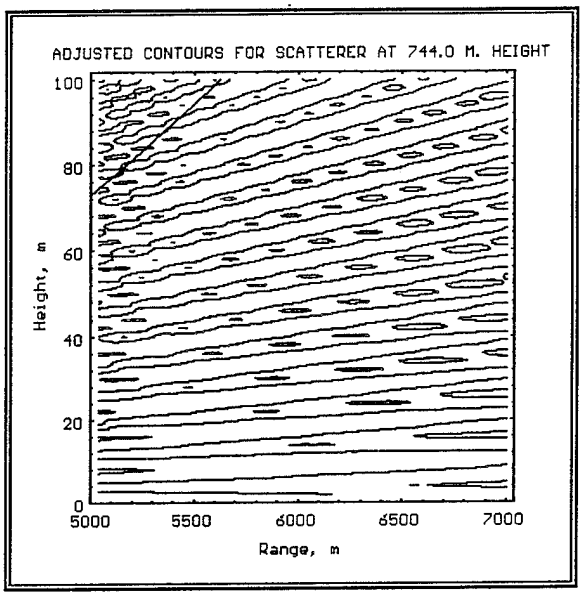

Figure 15. Adjusted scattered field (contours at −100, −105, and −110).

The direct field of figure 14 combined with the scattered field of figure 15 is shown in figure 16. The combination was accomplished by incoherent summation of the exitance values at each point, and then computing 10 times the common logarithm of the sum. The field depicted in figure 16 is representative only of the field to be expected in an actual battlefield scenario because of the assumptions made about the turbule number concentration spectrum and the angular dependence of the turbule scattering cross-section. The essential point to be made by the results shown in figure 16, which is the final goal of the work reported here, is that explicit description of the turbulence structure in terms of a turbule model, equation (1), and a turbule concentration has the potential for permitting calculation of scattered sound levels in shadow zones.

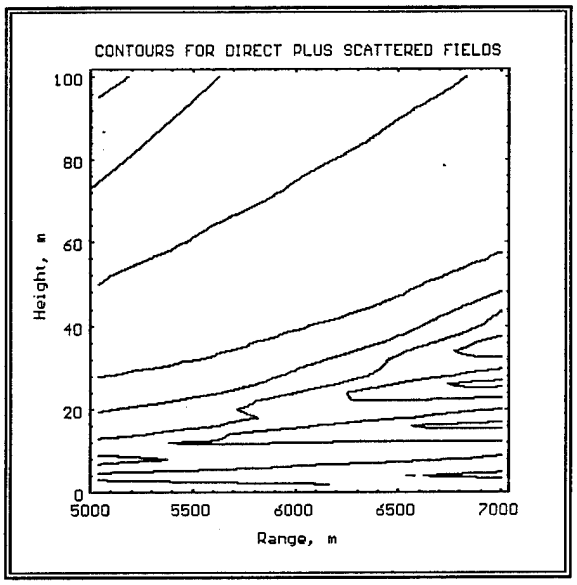

Figure 16. Combined primary and secondary scattered fields (contours at −80 to −110 in 5-db intervals).

5. Conclusions

This work, as reported, is part of the larger context of developing an acoustic propagation model that will be appropriate for future needs of the Army. These future needs include 20-km detection ranges, low frequencies, complex terrain, turbulence effects, and nonhomogeneous atmospheres. The initial objective of this development process is to determine if an explicit turbule scattering algorithm can be used to predict sound pressure levels in shadow zones that represent levels that have been measured in the field. This work with FFP and AMPP is intended to determine how far modification of existing propagation codes can be carried toward fulfilling future needs. As such, the scenario of figure 2 was selected as a compromise of all future needs to have something definite to work with. For investigation of the initial objective, a code was needed that exhibited a shadow zone. Unfortunately, a shadow zone at low frequencies does not have steep boundaries. Reasonable atmospheric parameters, such as sound speed gradient, will not produce dramatic and sharply defined shadow zones at low frequencies. On the other hand, as demonstrated in figure 7, calculations within shadow zones at multikilometer ranges produce results that at best cannot be interpreted and at worst are the result of loss of precision in computer operations. As a compromise measure to show something of the character of a shadow zone, the frequency was elevated to 170 Hz. To show a shadow zone at 10 Hz will require ranges of the full 20 km or greater. Thus, a fundamental limitation of the present propagation code has been identified. The next modification to be attempted is to provide for nonisotropic sources (and scatterers). Perhaps this step can be realized. But, the next step beyond, to go to the lower frequency and the longer range, cannot be accomplished unless modeling of sound pressure levels in shadow zones can be carried out to greater precision.

Left for future investigation is determination of a turbule number concentration distribution that is tied to a measurable turbulence intensity quantity such as the index-of-refraction structure parameter. Also left for future investigation is the turbule scattering cross section (and its angular dependance) at high size-to-wavelength ratios. AMPP has the capability of summing coherently the radiation from a moderate number of sources or scatterers. Summation from

a large number of turbules for a complete radiation field will take impossibly long. An analytical scheme needs to be devised, which will allow a natural collection of turbules to be represented by a moderate number of isotropic and anisotropic scattering centers. An investigation of this problem is the subject of a SBIR contract to be awarded soon.

References

1. Wolfram, S., *Mathematica A System for Doing Mathematics by Computer*, Second Edition, Addison-Wesley Publishing Company, Inc., Redwood City, CA, 1991.

2. Raspet, R., S. W. Lee, E. Kuester, D. C. Chang, W. F. Richards, R. Gilbert, and N. Bong, "A Fast-Field Program for Sound Propagation in a Layered Atmosphere Above an Impedance Ground," *J. Acoust. Soc. Am.*, 77(2), February 1985.

3. Brown, D. M., "Multiple Source and Scatterer Modification of the Fast Field Program Acoustics Propagation Model," Contractor Report (Draft), U.S. Army Atmospheric Sciences Laboratory, White Sands Missile Range, NM, 1992.

4. Goedecke, G. H., "Scattering of Acoustical Waves by a Spinning Atmospheric Turbule," CR-92-0001-2, U.S. Army Atmospheric Sciences Laboratory, White Sands Missile Range, NM, 1992.

5. Tatarskii, V. I., "The Effects of the Turbulent Atmosphere on Wave Propagation," TT-68-50464, National Technical Information Service, Springfield, VA, 1971.

6. Gilbert, K. E., R. Raspet, and Xiao Di, "Calculation of Turbulence Effects in an Upward-Refracting Atmosphere," *J. Acoust. Soc. Am.* 87(6), June 1990.

Acronyms and Abbreviations

AMPP	Acoustic Multistream Propagation Program
ARL	Army Research Laboratory
BED	Battlefield Environment Directorate
EPS	Encapsulated PostScript
FFP	Fast Field Program
PE	Parabolic Equation
SBIR	Small Business Innovative Research
SNR	signal-to-noise ratio
STAS	Short Term Analytical Services
WSMR	White Sands Missile Range

Appendix A

User Information for the AMPP

A-1. AMPP Output File Overview (outfiles.doc)

The following is a table of output files created by AMPP. The first entry is the file name. The convention 'nn' is used to show a two digit number is part of the file name. The first two digit number is the source number, the second, the detector number. Following the file name is a list of variables the file contains. A '/' designates a synonym for the first variable name. A ':' ends the table of synonyms and begins the description of the variables.

WAVNMOnn.nn
K / Xnew / Xold: Wave number
A / Ynew / Yold: Pressure

LEVELOnn.nn

R:	the range from zero
Level:	the db referenced to the free field case
Gain :	the db of the transmission loss

PROFILnn.nn

Idet:	the interface integer associated with a detector
Det:	the Z axis value of a detector
Isrc:	the interface integer associated with a source
Src:	the Z axis value of a source
C:	the speed of sound of a layer
Rho:	the Rho of a layer
Mu:	the Mu of a layer
Height:	the Z axis value of a layer
T:	the thickness of a layer

NPANEnn.nn

Kmax:	maximum K of the layers
Nyq:	the Nyquist number
Npan:	the number of panels
Kwidth:	wavenumber bandwidth of a panel
DeltaR:	incremental distance for range

DeltaK: incremental bandwidth

CLIPEnn.nn
K: wavenumber
LastN: identifier of a layer

WAVNMEnn.nn
K: wavenumber
REAL(A): real portion of the imaginary number associated with the pressure
IMAG(A): imaginary portion of the number associated with the pressure

PRESSEnn.nn
R: range
REAL(P): real portion of the pressure at that range
IMAG(P): imaginary portion of the pressure at that range

A-2. Creating a Detector File (mkdet.doc)

```
                    PROGRAM MKDET
C
C                   MKDET Operations Reference
C
C  MKDET was created to quickly make an AMPDETEC file.  It prompts the
C  user for the range in meters, the lowest detector height, the highest
C  detector height, and how many detectors there are in the model.  The
C  program will then write out an AMPDETEC type file named
C  AMPDETEC.NEW.
C
      INTEGER  REPS
      REAL     RANGE,ZBEG,ZEND,Z,DELTAZ
C
      WRITE(*,*) "Please enter the range :"
      READ(*,*) RANGE
      WRITE(*,*) "Enter the height of the first detector :"
      READ(*,*) ZBEG
```

```
      WRITE(*,*) "Enter the height of the last detector :"
      READ(*,*) ZEND
      WRITE(*,*) "Enter the number of detectors :"
      READ(*,*)REPS
      DELTAZ = (ZEND - ZBEG) / (REPS - 1.0)
      OPEN(11,FILE="ampdetec.new",STATUS="UNKNOWN")
      WRITE(11,*) REPS
      DO     20  Z =ZBEG,ZEND,DELTAZ
             WRITE(11,10) RANGE,0.0,Z
10           FORMAT (2X,3(E12.5E2,1X))
20    CONTINUE
      END
```

A-3. Creating a layer file (amplayer.doc)

Instructions on MET and MENU3 (how to make AMPLAYER files)

To make an AMPLAYER file, one must run two programs: MET and MENU3. The following is a discussion on how to do that:

MET:
The program expects a met-file to be named W.IN (Weather input). To execute the program type MET, it will then write a file readable by MENU3 called MET.OUT. Table A-1 is an example of W.IN.

Table A-1. An example of W.IN. The data in the file is from measurements taken in 1989 at White Sands Missile Range C Station. The format is in the style used by ARL as input to other acoustic models

Height (m)	Temp (K)	Rel Hum (%)	Press (atm)	Wind Speed (m/s)	Wind Dir (rad)
0.00	301.350	41.000	.868	3.089	1.484
3.35	301.250	41.000	.868	3.089	1.484
64.31	300.050	41.000	.862	2.574	1.536
125.27	298.850	42.000	.856	2.574	1.588
186.23	297.750	43.000	.850	2.059	1.658
247.19	296.550	43.000	.844	2.059	1.745
308.15	295.450	44.000	.838	2.059	1.815
369.11	294.850	45.000	.832	1.544	1.920
430.07	294.350	47.000	.826	1.544	2.025
491.03	293.850	47.000	.820	1.544	2.129
551.99	293.350	47.000	.815	1.544	2.217
612.95	293.050	47.000	.809	1.544	2.286
673.91	292.750	47.000	.803	1.544	2.356
734.87	292.350	48.000	.798	1.544	2.426
795.83	291.750	50.000	.792	1.544	2.496
856.79	291.150	51.000	.786	1.544	2.548
917.75	290.650	52.000	.781	1.544	2.601
978.71	290.250	53.000	.775	2.059	2.635
1039.67	290.150	55.000	.770	2.059	2.688
1100.64	290.050	56.000	.764	2.059	2.740

Table A-1. An example of W.IN. The data in the file is from measurements taken in 1989 at White Sands Missile Range C Station. The format is in the style used by ARL as input to other acoustic models (continued)

Height (m)	Temp (K)	Rel Hum (%)	Press (atm)	Wind Speed (m/s)	Wind Dir (rad)
1161.59	289.950	56.000	.759	2.059	2.793
1222.56	289.750	56.000	.754	2.574	2.862
1283.52	289.550	57.000	.748	2.574	2.932
1344.48	289.350	57.000	.743	2.574	3.002
1405.44	288.950	58.000	.738	2.574	3.072
1466.40	288.450	60.000	.732	2.574	3.159
1527.36	287.950	61.000	.727	2.574	3.246
1588.32	287.750	54.000	.722	2.574	3.316
1649.28	287.650	46.000	.717	2.754	3.386
1710.24	287.250	43.000	.712	2.574	3.438
1771.20	286.750	44.000	.706	2.574	3.491
1832.16	286.250	45.000	.701	3.089	3.526
1893.12	285.650	47.000	.696	3.089	3.508
1954.08	285.150	49.000	.691	2.574	3.508
2015.04	284.450	51.000	.686	2.574	3.526
2076.00	283.850	52.000	.681	2.574	3.560
2136.96	283.250	55.000	.676	2.574	3.578
2197.92	282.650	57.000	.671	2.574	3.613
2258.88	282.150	59.000	.666	2.574	3.648
2319.84	281.550	61.000	.662	2.059	3.700
2380.80	280.950	63.000	.657	2.059	3.735
2441.76	280.350	65.000	.652	2.059	3.683
2502.72	279.750	66.000	.647	2.059	3.630
2563.68	279.250	63.000	.642	2.059	3.752
2624.64	278.650	60.000	.638	1.544	3.892
2685.60	278.350	51.000	.633	1.544	3.962
2746.56	278.150	37.000	.628	1.544	3.962
2807.52	278.050	24.000	.623	1.544	3.979
2868.48	278.050	19.000	.619	1.544	3.979
2929.44	277.950	14.000	.614	1.544	3.962
2990.40	277.950	10.000	.610	1.544	3.892

Table A-2 is an example of MET.OUT produced from the above W.IN file with wind direction of 0.0 degrees.

Table A-2. An example of MET.OUT produced from the W.IN file with wind direction of 0.0 °

H (m)	Wspeed (m/s)	WinDgr (°)	Tempc (°C)	Relhum (%)	PO (mb)	Walong (m/s)	Speed (m/s)
3.35	3.1	85.0	28.1	41.0	879.5	-.3	3.1
64.31	2.6	88.0	26.9	41.0	873.4	-.1	2.6
125.27	2.6	91.0	25.7	42.0	867.3	.0	2.6
186.23	2.1	95.0	24.6	43.0	861.3	.2	2.1
247.19	2.1	100.0	23.4	43.0	855.2	.4	2.1
308.15	2.1	104.0	22.3	44.0	849.1	.5	2.1
369.11	1.5	110.0	21.7	45.0	843.0	.5	1.5
430.07	1.5	116.0	21.2	47.0	836.9	.7	1.5
491.03	1.5	122.0	20.7	47.0	830.9	.8	1.5
551.99	1.5	127.0	20.2	47.0	825.8	.9	1.5
612.95	1.5	131.0	19.9	47.0	819.7	1.0	1.5
673.91	1.5	135.0	19.6	47.0	813.6	1.1	1.5
734.87	1.5	139.0	19.2	48.0	808.6	1.2	1.5
795.83	1.5	143.0	18.6	50.0	802.5	1.2	1.5
856.79	1.5	146.0	18.0	51.0	796.4	1.3	1.5
917.75	1.5	149.0	17.5	52.0	791.3	1.3	1.5
978.71	2.1	151.0	17.1	53.0	785.3	1.8	2.1
1039.67	2.1	154.0	17.0	55.0	780.2	1.9	2.1
1100.64	2.1	157.0	16.9	56.0	774.1	1.9	2.1
1161.59	2.1	160.0	16.8	56.0	769.1	1.9	2.1
1222.56	2.6	164.0	16.6	56.0	764.0	2.5	2.6
1283.52	2.6	168.0	16.4	57.0	757.9	2.5	2.6
1344.48	2.6	172.0	16.2	57.0	752.8	2.5	2.6
1405.44	2.6	176.0	15.8	58.0	747.8	2.6	2.6

Table A-2. An example of MET.OUT produced from the W.IN file with wind direction of 0.0 ° (continued)

H (m)	Wspeed (m/s)	WinDgr (°)	Tempc (°C)	Relhum (%)	PO (mb)	Walong (m/s)	Speed (m/s)
1466.40	2.6	181.0	15.3	60.0	741.7	2.6	2.6
1527.36	2.6	186.0	14.8	61.0	736.6	2.6	2.6
1588.32	2.6	190.0	14.6	54.0	731.6	2.5	2.6
1649.28	2.6	194.0	14.5	46.0	726.5	2.5	2.6
1710.24	2.6	197.0	14.1	43.0	721.4	2.5	2.6
1771.20	2.6	200.0	13.6	44.0	715.4	2.4	2.6
1832.16	3.1	202.0	13.1	45.0	710.3	2.9	3.1
1893.12	3.1	201.0	12.5	47.0	705.2	2.9	3.1
1954.08	2.6	201.0	12.0	49.0	700.0	2.4	2.6
2015.04	2.6	202.0	11.3	51.0	695.1	2.4	2.6
2076.00	2.6	204.0	10.7	52.0	690.0	2.4	2.6
2136.96	2.6	205.0	10.1	55.0	685.0	2.3	2.6
2197.92	2.6	207.0	9.5	57.0	679.9	2.3	2.6
2258.88	2.6	209.0	9.0	59.0	674.8	2.3	2.6
2319.84	2.1	212.0	8.4	61.0	670.8	1.7	2.1
2380.80	2.1	214.0	7.8	63.0	665.7	1.7	2.1
2441.76	2.1	211.0	7.2	65.0	660.6	1.8	2.1
2502.72	2.1	208.0	6.6	66.0	655.6	1.8	2.1
2563.68	2.1	215.0	6.1	63.0	650.5	1.7	2.1
2624.64	1.5	223.0	5.5	60.0	646.5	1.1	1.5
2685.60	1.5	227.0	5.2	51.0	641.4	1.1	1.5
2746.56	1.5	227.0	5.0	37.0	636.3	1.1	1.5
2807.52	1.5	228.0	4.9	24.0	631.3	1.0	1.5
2868.48	1.5	228.0	4.9	19.0	627.2	1.0	1.5
2929.44	1.5	227.0	4.8	14.0	622.1	1.1	1.5
2990.40	1.5	223.0	4.8	10.0	618.1	1.1	1.5

MENU3:

MENU3 was written to help make input files for the program FFP. The following are the steps to take to make a file for AMPP.

1. Execute the program by typing MENU3.
2. Select "4. Atmospheric Profile"
3. Select "5. Read a weather profile"
4. Enter the file name "MET.OUT"
5. Select "0. Done"
6. Select "5. Atmospheric Layering"
7. Follow directions from program.
8. Select "0. Done"
9. Select "12. Write an FFP input file" giving any filename.
10. Select "0. Done"

You now have a file you picked in step 9. Before using this file with AMPP, you must edit it with any editor you have on-line. The following is an example of the file MENU3 produces. Text in brackets, [ ], are my notes on how to edit the file.

MENU3 Example Output

```
1.60000E+02    , Frequency
1.80000E+00  1.50000E+00 , Source,Detector Height
1.00000E+02    , Maximum Det. Range
( 1.17E+01,-1.40E+01) ( 1.00E+06, 0.00E+00)  , Zc1,Kc1
( 1.00E+00, 0.00E+00) ( 1.00E+00, 0.00E+00)  , ZcN,KcN
-2             , Npan
1024           , Points
1.00000E-03    , Extra
1.00000E+08    , Exp. of Kzmax

2              , Output [Delete this and all previous lines]

0.00000E+00 3.41097E+02 1.20000E+00 8.00001E-05
1.00000E+01 3.41085E+02 1.20000E+00 8.00016E-05
```

2.00000E+01 3.41061E+02 1.20000E+00 8.00044E-05
3.00000E+01 3.41037E+02 1.20000E+00 8.00069E-05
4.00000E+01 3.41013E+02 1.20000E+00 8.00090E-05
5.00000E+01 3.40989E+02 1.20000E+00 8.00109E-05
6.00000E+01 3.40965E+02 1.20000E+00 8.00126E-05
7.00000E+01 3.40942E+02 1.20000E+00 8.00139E-05
8.00000E+01 3.40918E+02 1.20000E+00 8.00150E-05
9.00000E+01 3.40894E+02 1.20000E+00 8.00158E-05
1.00000E+02 3.40870E+02 1.20000E+00 8.00163E-05
0.00000E+00 3.40858E+02 1.20000E+00 8.00164E-05

Once you have deleted the lines, count the remaining non-blank lines. Insert that number at the top of the file. The columns are:

Height (m)	SSpeed (m/s)	Density (kg/m^3)	Absorption (nepers/m)

The height is for the bottom of the layer. An example follows:

Example of AMPLAYER File

12
0.00000E+00 3.41097E+02 1.20000E+00 8.00001E-05
1.00000E+01 3.41085E+02 1.20000E+00 8.00016E-05
2.00000E+01 3.41061E+02 1.20000E+00 8.00044E-05
3.00000E+01 3.41037E+02 1.20000E+00 8.00069E-05
4.00000E+01 3.41013E+02 1.20000E+00 8.00090E-05
5.00000E+01 3.40989E+02 1.20000E+00 8.00109E-05
6.00000E+01 3.40965E+02 1.20000E+00 8.00126E-05
7.00000E+01 3.40942E+02 1.20000E+00 8.00139E-05
8.00000E+01 3.40918E+02 1.20000E+00 8.00150E-05
9.00000E+01 3.40894E+02 1.20000E+00 8.00158E-05
1.00000E+02 3.40870E+02 1.20000E+00 8.00163E-05
0.00000E+00 3.40858E+02 1.20000E+00 8.00164E-05

Notice there were twelve lines of data; therefore, the integer 12 was placed at the top of file. Save the file as AMPLAYER and the process is complete.

An alternate method was used to generate the AMPLAYER file for the input data used in this report. A option file MENU3OPT.1 was read into MENU3 and some changes made in the options. The parameters may be determined where MENU3OPT.1 is reproduced below. The procedure used was as follows:

1.	MENU3	[Execute program MENU3]
2.	(10)	[Read in an option file]
3.	MENU3OPT.1	[Option file name]
4.	(4)	[Atmospheric profile]
5.	(3)	[Sound Speed profile]
6.	(1)	[Linear profile]
7.	335.1	[Lower height sound speed]
8.	331.399	[Upper height sound speed]
9.	(0)	[Quit atmospheric profile]
10.	(12)	[Write a FFP input file]
11.	MET.OUT	[File name]
12.	(0)	[Quit MENU3]

The above procedure for converting MET.OUT into AMPLAYER was then used. This procedure produced a linear sound speed gradient that corresponded to a ground temperature of 4.957 °C and a temperature at 1 km of −1.1524 °C. The attenuation coefficient, then, would be about 10 percent low for this temperature range. This would cause a level change from −.393 to −.354 db at 7000 m caused by molecular absorption. This small change will not materially effect the results. For the purposes of this report, it was not considered cost effective to recalculate the data when this inconsistency was discovered. MENU3OPT.1 is reproduced below.

1,Src,Det,R [Main Menu]

1.00000E+01,	Source height (m)
1.01000E+01,	Detector height (m)
1.00000E+04,	Maximum range (m)

2, Npan,Points,Extra,Ekzmax,Output [Main Menu]

−2,	Number of FFT panels
1024,	Points per FFT
1.00000E-05,	Extra loss
1.00000E+08,	Maximum vertical decay
2,	FFP output flag

3, Ground impedance [Main Menu]

3,	Attenborough 4-parameter model
2.00000E+05,	Flow resistivity
8.75000E-01,	Pore shape factor ratio
4.00000E-01,	Measured (volume) porosity
7.50000E-01,	Grain shape factor
1,	Local reaction

4, Atmospheric profiles [Main Menu]

1,	Temperature profile
0.00000E+00,	Surface temperature
1,	Linear function
1.50000E+01,	Height of section
-9.00000E-02,	Temp at top of section
-6.00000E-03,	Slope of the section
1,	Linear function
3.00000E+01,	Height of section
-1.80000E-01,	Temp at top of section
-6.00000E-03,	Slope of the section
1,	Linear function
9.00000E+01,	Height of section
-5.40000E-01,	Temp at top of section
-6.00000E-03,	Slope of the section
1,	Linear function
1.20000E+02,	Height of section
-7.20000E-01,	Temp at top of section
-6.00000E-03,	Slope of the section
1,	Linear function
1.50000E+02,	Height of section

-9.00000E-01,	Temp at top of section
-6.00000E-03,	Slope of the section
1,	Linear function
1.80000E+02,	Height of section
-1.08000E+00,	Temp at top of section
-6.00000E-03,	Slope of the section
0,	Done with temp profile
4,	Air absorption
1,	Temp profile used for alpha
8.00000E+01,	Relative humidity
0,	Done with atmosphere menu

5, Atmospheric layering [Main Menu]

1,	Uniform layering
1.00000E+03,	Height of profile
60,	Number of layers
0,	Done with layering routine

6, Frequencies [Main Menu]

1,	Single frequency
1.70000E+02,	Frequency (Hz)

A-4. Compiling AMPP Source Files (compile.doc)

Fortran Compilation

From the menu press PgDn and the function key next to the Fortran entry. That will get you to the correct directory. Type ENTER and press return. That will setup the environment for you. Type FL followed by the filename of the program to be compiled. Ensure you type the .FOR extender. The program will then be compiled and linked, creating a file with the same name but with an .EXE extender. To exit, type MENU and press return.

From the menu press PgDn and the function key next to the C++ entry. To exit press ALT X. It automatically returns you to the menu.

A-5. AMPP Input Files Overview (infiles.doc)

File: AMPINPUT

```
&INPUTS
F        = 1.70000E+02
Zc1      = ( 1.07E+01,-1.00E+01)
Kc1      = ( 1.00E+06, 0.00E+00)
ZcN      = ( 1.00E+00, 0.00E+00)
KcN      = ( 1.00E+00, 0.00E+00)
Npan     = -2
Points   = 1024
Extra    = 5.00E-05
Ekzmax   = 1.00E+08
Output   = -1
BW       = 1.00000E-06
Ncoher   =1
/
```

The first and last lines are for the MS Fortran namelist convention. All other lines are self explanatory.

File: AMPLAYER

```
62
0.00000E+00 3.35100E+02 1.20000E+00 6.05352E-05
1.66667E+01 3.35069E+02 1.20000E+00 6.04696E-05
.....
1.00000E+03 3.31430E+02 1.20000E+00 5.18718E-05
0.00000E+00 3.31399E+02 1.20000E+00 5.18065E-05
```

The first line is the number of layers. Each layer has the following variables associated with if, from left to right:

Z : top height of the layer
C : speed of sound of the layer
Rho: Rho of the layer
Mu: Mu of the layer

NOTE: the "....." represent 58 similar lines.

File: AMPSOURC

```
1
5.00000E+03 0.00000E+00 9.95000E+02 0.7853982
```

The first line is the number of sources. Each line after represents a source with the following variables:

R: range in meters on the X axis.
Y: not used.
Z: range in meters on the Z axis.
P: relative phase of the source to all other sources.

File: AMPDETEC

```
5
.10000E+05   .00000E+00   .11000E+01
.10000E+05   .00000E+00   .31184E+01
.10000E+05   .00000E+00   .51367E+01
.10000E+05   .00000E+00   .71551E+01
.10000E+05   .00000E+00   .91735E+01
```

The first line is the number of detectors. Each line after represents a detector with the following variables:

R: range in meters on the X axis.
Y: not used.
Z: range in meters on the Z axis.

File: AMPSCATT

1
5.00000E+03 0.00000E+00 9.95000E+02 0.7853982

The first line is the number of scatterers. Each line after represents a scatterer with the following variables:

R: range in meters on the X axis.
Y: not used.
Z: range in meters on the Z axis.
P: not used.

Appendix B

Spherical Propagation Program

The Spherical program calculates the acoustic exitance ($w \cdot m^{-2}$) field for a uniform atmosphere above a flat ground plane modeled as a locally reacting porous medium impedance discontinuity.* The impedance is calculated in subroutine ZEE.† The representation of the complementary error function is calculated in subroutine W.

```
C     PROGRAM SPHERICAL
C
C     THIS PROGRAM OBTAINED FROM JOHN NOBLE CALCULATES THE ACOUSTIC
C     FIELD FOR A SPHERICAL WAVE WITH A FLAT BOUNDARY.  MODIFICATIONS
C     BEGUN 16 OCT., 1991 BY HARRY J. AUVERMANN.  LATEST MODIFICATIONS
C     21 OCT., 1991.
C
      real fr,K,mzr,ZR,ZS,SIG,Ra,R1,R2,TL(50,50),TLZ00(50)
      real COSE
      complex PESQ,PE,Z,wiz,AMP
      complex FPE,REFL,ZC,i
      character*64 fname
C     constants
      data PI/3.14159265/
      print*,"Name of output file"
      read*,fname
      open(unit=11,file=fname)
      open(unit = 12, file = 'param.dat')
      WRITE(11,2001)
      WRITE(12,2001)
      i=(0.,1.)
      print *,"Temperature in C"
      read (*,*) T
      C = 331.6
      C0 = C * sqrt(1 + T / 273.15)
      print *,"Sigma:"
      read (*,*) sig
      SIG=sig*1000.
      print *,"Frequency:"
      read (*,*) Fr
      K=2.0*PI*fr/C0
C
      print *,"Source Height"
      read (*,*) Zs
      print *,"Maximum Receiver Height"
      read (*,*) MZr
```

* Attenborough, K., S. I. Hayek, and J. M. Lawther, "Propagation of Sound Above a Porous Half-Space," *J. Acoust. Soc. Am.* 68(5), Nov. 1990.

† Delany, M. E. and E. N. Bazley, "Acoustical Properties of Fibrous Absorbent Materials," *Appl. Acoust.* 3, 1970, pp. 105-116.

```
      print *, "Minimum Receiver Height"
      read (*,*) z0
      print *,"Maximum Range:"
      read (*,*) Rmax
      print *, "Minimum Range:"
      read (*,*) r0
      nr = 50
      nz = 50
      dr = (Rmax - r0) / nr
      dz = (mzr - z0) / nz
      IR = 1
      sdf=sig/fr
      call  ZEE(SDF,ZC)
C
      write (11,*) nz
      write (11,*) (z0+j*dz,j=1,nz)
      IZ0 = 0
10    continue
      IF(IZ0 .EQ. 0) THEN
      ZR = 0.0
      NRL = NR
      NZL = 1
      RA = R0 + IR*DR
      ELSE
      NRL = NR
      NZL = NZ
      RA = R0 + IR*DR
      END IF
      do 20 iz = 1, NZL
      IF(IZ0 .NE. 0) ZR = Z0 + IZ*DZ
C     distance from source to receiver.
      R1=sqrt(Ra**2+(ZR-ZS)**2)
C     distance from image to receiver.
      R2=sqrt(Ra**2+(ZR+ZS)**2)
C     cosine of theta
      COSE=(ZR+ZS)/R2
C
      REFL=(COSE-1./ZC)/(COSE+1./ZC)
      PESQ=.5*i*K*R2*(COSE+1./ZC)**2
      PE=csqrt(PESQ)
      Z=-i*PE
      call w(Z,wiz)
      FPE=1.+i*sqrt(PI)*PE*wiz
      AMP=cexp(i*K*R1)/R1
     2  +(REFL+(1.-REFL)*FPE)*cexp(i*K*R2)/R2
C
      IF(IZ0 .EQ. 0) THEN
      TLZ00(IR) = 20*alog10(cabs(amp))
      ELSE
      TL(IR,IZ)=20*alog10(cabs(amp))
      END IF
```

```
C
      zr=zr+dz
20    continue
C     write (11,*) ra,(tl(j),j=1,nz)
      IF(IZ0 .EQ. 0) THEN
      IR = IR + 1
      IF (IR .LE. NRL) goto 10
      ZR = Z0
      IR = 0
      IZ0 = 20
      END IF
      IR = IR + 1
      IF (IR .LE. NRL) goto 10
      DO 30 JZ = 1, NZ
      WRITE(11,2003) (TL(JR,JZ), JR = 1, 5)
      WRITE(11,2004) (TL(JR,JZ), JR = 6, 45)
      WRITE(11,2005) (TL(JR,JZ), JR = 46, NZ)
30    CONTINUE
C
      WRITE(11,2002)
C     WRITE OUT PARAMETER INFORMATION
      RA = R0 + DR
      ZA = Z0 + DZ
      WRITE(12,2012) RA, ZA, TL(1,1)
      WRITE(12,2010)
      WRITE(12,2011) T,C0,SIG,FR,ZS,MZR,Z0,RMAX,R0,NR,NZ,ZC
      WRITE(12,2013)
      WRITE(12,2014) (TLZ00(JJ), JJ = 1, 50)
      WRITE(12,2002)
C
150   stop
2001  FORMAT(5X,'BEGIN PROGRAM SPHERICAL')
2002  FORMAT(5X,'FINIS PROGRAM SPHERICAL')
2003  FORMAT(2X,'{',5(1PE13.6,', '))
2004  FORMAT(7(3X,5(1PE13.6,', '),/),3X,5(1PE13.6,', '),)
2005  FORMAT(3X,4(1PE13.6,', '),1PE13.6,' },')
2010  FORMAT(2X,'TEMPERATURE',4X,'SOUND',7X,'SIGMA',5X,'FREQUENCY',
     A  4X,'SOURCE',5X,
     2' MAXIMUM',3X,'MINIMUM',3X,'MAXIMUM',3X,'MINIMUM',3X,
     3  'NUM.',3X,'NUM.',7X,'INTERFACE',/,
     4  4X,'DEGREES',5X,'VELOCITY',2X,10X,5X,'HERTZ',6X,'HEIGHT',5X,
     5  'RECEIVER',2X,'RECEIVER',3X,'RANGE',5X,'RANGE',3X,'RANGE',2X,
     6  'HEIGHT',6X,'IMPEDANCE',/,
     7  4X,'CELSIUS',7X,'M/S',8X,5X,4X,4X,5X,8X,'M',7X,'HEIGHT',4X,
     8  'HEIGHT',7X,'M',9X,'M',4X,'INCREM.',1X,
     9  'INCREM.',7X,'RATIO',/)
2011  FORMAT(2X,5(1PE11.4,1X),4(1PE9.2,1X),
     2  2(I4,3X),2(1PE9.2,1X))
2012  FORMAT(2X,'CALCULATED LEVEL AT RANGE ',1PE11.4,' M. AND HEIGHT
     ',
     2  1PE11.4,' M. IS ',1PE11.4)
```

```
2013  FORMAT(/,2X,'CALCULATED LEVELS AT ZERO HEIGHT ARE:',/)
2014  FORMAT(5(2X,10(1PE11.4,1X),/))
      end
C
C     DELANY-BAZELY
      subroutine ZEE(SDF,ZC)
      COMPLEX ZC,i
      i=(0.,1.)
      TWOPI=6.28318531
      ZC=1.+.05*SDF**0.75+i*0.077*SDF**0.73
      return
      end
C
      subroutine w(z,wiz)
      logical lx,ly
      complex z,wiz,cefw,s,t1,t2,t3
      data cons/1.128379167095/
      x=-aimag(z)
      y=real(z)
C
      x1=y
      y1=-x
C
C     determine quadrant for z
C
10    lx=x.ge.0.0
      ly=y.ge.0.0
      if(lx.and.ly)iq=1
      if(.not.lx.and.ly)iq=2
      if(.not.lx.and..not.ly)iq=3
      if (lx.and..not.ly)iq=4
C
C     convert to first quadrant
C
      x=abs(x)
      y=abs(y)
      s=cmplx(x,y)
      xs=x
      ys=y
C
100   if(y.ge.4.29.or.x.ge.5.33) go to 110
      s=(1.0-y/4.29)*sqrt((1.0-(x*x)/28.41))
      h=1.6*s
      h2=2.0*h
      ncap=6.5+23.0*s
      alamda=h2**ncap
      nu=9.5+21.0*s
      go to 120
110   t1=4.613135e-1/(s*s-1.901635e-1)
      t2=9.999216e-2/(s*s-1.7844927)
      t3=2.883894e-3/(s*s-5.5253437)
```

```
      wiz=s*(t1+t2+t3)
      v=real(wiz)
      u=-aimag(wiz)
      go to 180
120   r1=0.0
      r2=0.0
      s1=0.0
      s2=0.0
      n=nu
130   if(n.lt.0) go to 150
      p1=n+1
      t1=y+h+p1*r1
      t2=x-p1*r2
      c=0.5/(t1*t1+t2*t2)
      r1=c*t1
      r2=c*t2
      if(h.eq.0.0.or.n.gt.ncap) go to 140
      t1=alamda+s1
      s1=r1*t1-r2*s2
      s2=r2*t1+r1*s2
      alamda=alamda/h2
140   n=n-1
      go to 130
150   if(alamda.eq.0.0) go to 160
      u=cons*s1
      v=cons*s2
      go to 180
160   u=cons*r1
      v=cons*r2
180   cefw=cmplx(u,v)
C
C     test for underflow and overflow
C
      test=-xs*xs+ys*ys
      if(test.lt.-85.0)test=-85.0
      if(test.gt.87.)test=87.0
C     test for quadrant
      go to(230,220,210,210),iq
210   cefw=2.0*cexp(cmplx(test,-2.*xs*ys))-cefw
      if(iq.eq.3) go to 230
      if(iq.eq.4) go to 220
C     for 2nd and 4th quadrants conjugate cefw
C
220   cefw=conjg(cefw)
230   wiz=cefw
      return
      end
```

The above code receives interactive input on FORTRAN unit 11. Quantities required as input and typical values are listed below:

Quantity	Typical Value
Temperature	5.8 (°C)
SIGMA	134.0 (porosity parameter)
Frequency	170.0 (Hz)
Source Height	10.0 (m)
Maximum Receiver Height	200.0 (m)
Minimum Receiver Height	0.0 (m)
Maximum Range	7000.0 (m)
Minimum Range	5000.0 (m)

Output is sent to unit 12 and the file PARAM.DAT.

Appendix C

Limitray Program

The limit ray as described in this report is the path traveled by a ray in an atmosphere with a uniform sound speed gradient with the sound speed decreasing with increasing altitude. This path has been proven to be a circle.* The limit ray circle passes through the source and is tangent to the ground surface. Below, the equations satisfied by the ray path under these conditions are developed in section 1, and the code written to obtain tables of path coordinates is included in section 2.

C-1. Ray Path Theory

The center point and radius of the limit ray circle are calculated relative to the diagram of figure C-1.

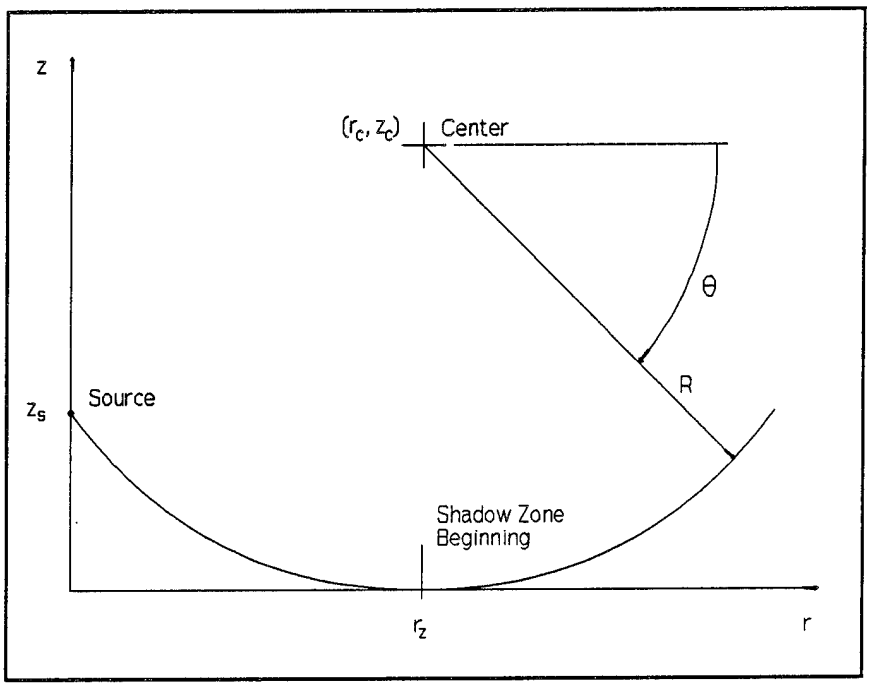

Figure C-1. Limit ray geometry.

* Dowling, A. P. and J. E. Ffowcs-Williams, *Sound and Sources of Sound*, Ellis Horwood Limited, Chichester, 1983.

Definition of the symbols to be used below and in the diagram are as follows:

r	=	range coordinate
z	=	height coordinate
g	=	sound speed gradient, $(m \cdot s^{-1})/m$
c_0	=	sound speed at ground level
r_c	=	range coordinate of circle center
z_c	=	height coordinate of circle center
z_s	=	height of source
r_z	=	range coordinate of beginning of shadow zone
R	=	circle radius
R'	=	radius of a concentric circle
ΔR	=	$R - R'$
$c(R')$	=	sound velocity at radius R' with $\theta = \pi/2$
θ	=	angle from horizontal of radius vector to a path point
r_1	=	range coordinate of a path point
z_1	=	height coordinate of a path point

For the case when $\theta = -\pi/2$, the radius vector is vertical and the phase front of the wave is vertical also. To maintain a phase front that passes through the circle center, it is necessary that the ray traveling on a circle of radius slightly less than R travel a distance less than the ray on the limit circle. If $\Delta\theta$ is the arc subtended by the limit ray in a small time Δt, then this same angle is subtended by the ray on the circle of radius $R' = R - \Delta R$. Thus

$$\Delta\theta = (c_0\ \Delta t)/R = (c(R-\Delta R)\ \Delta t)\ /\ (R-\Delta R), \tag{C-1}$$

or

$$c_0/R = c(R-\Delta R)/(R-\Delta R). \tag{C-2}$$

The sound speed at the second location is the sound speed at the limit ray position plus the gradient times the radius change or

$$c(R-\Delta R) = c_0 + g\ \Delta R. \tag{C-3}$$

When equation (C-3) is substituted in equation (C-2), the result is

$$g = -c_0/R. \tag{C-4}$$

Given g and c_0, R is determined. The remaining quantities are determined from the geometry of figure C-1. These are

$$z_c = R = -c_0/g, \tag{C-5}$$

$$r_c = [R^2-(z_s+c_0/g)^2]^{1/2}, \tag{C-6}$$

and

$$r_z = r_c.$$

Bringing all the relations together, the expression for the limit ray height as a function of the limit ray range is

$$z_1/R = 1 - [1-(r_1 - r_z)^2/R^2]^{1/2}, \tag{C-7}$$

and

$$z_1 = R\ \{1 - [1 - (r_1 - r_z)^2/R^2]^{1/2}\}. \tag{C-8}$$

Equation (C-8) is evaluated in the Spherical program which is recorded in the next section.

C-2. Limitray Source Code Listing

The following is a listing of the Fortran source code for Program Limitray developed using MS-DOS Fortran, Version 5.0.

```
C     PROGRAM LIMITRAY
C
C     THIS PROGRAM OBTAINED FROM JOHN NOBLE CALCULATES THE
C     SHADOW ZONE BOUNDARY RAY IN AN ATMOSPHERE THAT HAS A
C     UNIFORM SOUND VELOCITY GRADIENT.  LAST MODIFIED BY HARRY J.
C     AUVERMANN ON 19 DEC., 1991.
C
C     VARIABLES
C
C     G  = SOUND VELOCITY GRADIENT, M*S**-1, (NEGATIVE IF SOUND
C     VELOCITY ALOFT IS SLOWER THAN AT GROUND LEVEL)
C     ZS = SOURCE HEIGHT, M
C     C0 = GROUND LEVEL SOUND VELOCITY
C     D  = HORIZONTAL RANGE AT WHICH HEIGHT OF BOUNDARY IS DESIRED
C     (D WAS AN INPUT QUANTITY IN THE ORIGINAL VERSION.  IN
C     THIS VERSION, AN INTERVAL AND AN INCREMENT IS INPUT
C     SO THAT AN ARRAY OF BOUNDARY POINTS IS CALCULATED)
C     DL = LOWER LIMIT OF HORIZONTAL RANGE
C     DU = UPPER LIMIT OF HORIZONTAL RANGE
C     DD = HORIZONTAL RANGE INCREMENT
C     ND = NUMBER OF HORIZONTAL RANGE INCREMENTS TO BE CALCULATED
C     CS = SOUND VELOCITY AT SOURCE HEIGHT
C     D0 = HORIZONTAL DISTANCE TO RAY MINIMUM POINT
C     ZSH   = ARRAY OF HORIZONTAL DISTANCES AND RAY HEIGHTS
C
      IMPLICIT REAL (A-Z)
      DIMENSION ZSH(200,2)
C
      WRITE(*,*) "Enter sound speed gradient"
      READ(*,*)  G
      WRITE(*,*) "Enter height of the source"
      READ(*,*)  ZS
      WRITE(*,*) "Enter sound speed at ground level"
      READ(*,*)  C0
      WRITE(*,*) "Enter lower limit of range interval"
      READ(*,*)  DL
      WRITE(*,*) "Enter upper limit of range interval"
      READ(*,*)  DU
      WRITE(*,*) "Enter range increment"
      READ(*,*)  DD
C
C     -----Calculate the range to the start of the shadow zone
      CS = C0 + G*ZS
```

```
      D0 = SQRT(ZS*ZS - 2.0*CS*ZS/G)
C
C     -----Calculate height of the limit ray at the ranges of interest
      ND = INT((DU - DL)/DD) + 1
      DO 10 ID = 1, ND
      D = DL + (ID - 1)*DD
      ZSH(ID,1) = D
      ZSH(ID,2) = ZS - SQRT(CS*CS/(G*G) + 2.0*D*D0 - D*D) - CS/G
      IF(D .LT. D0) THEN
      WRITE(*,*) "RANGE D = ",D," IS NOT IN THE SHADOW ZONE"
      END IF
   10 CONTINUE
C
C     -----Print the results
      WRITE(*,*) " "
      WRITE(*,*) "========================================="
      WRITE(*,*) "Shadow zone begins at ",D0," meters"
      WRITE(*,*) "Limit ray coordinates"
      WRITE(*,*) "     Range           Height"
      WRITE(*,*) "     Meters          Meters"
      WRITE(*,*) ("     ",ZSH(JD,1),ZSH(JD,2), JD = 1, ND)
C
      OPEN(UNIT = 12, FILE = 'LIMITRAY.DAT')
      WRITE(12,*) "     LIMIT RAY COORDINATES"
      WRITE(12,*) "     Sound speed gradient is ",G ," meters/second"
      WRITE(12,*) "     Source height is        ",ZS," meters"
      WRITE(12,*) "     Ground sound speed is   ",C0," meters"
      WRITE(12,*) "     Shadow zone begins at   ",D0," meters"
      WRITE(12,*) "     Range           Height"
      WRITE(12,*) "     Meters          Meters"
      WRITE(12,2003) (ZSH(JD,1),ZSH(JD,2), JD = 1, ND - 1)
      WRITE(12,2004) ZSH(ND,1),ZSH(ND,2)
C
      STOP
2003  FORMAT( 3X,'{{',1PE13.6,',',5X,1PE13.6,' },',/,
     2  58(3X,' {',1PE13.5,',',5X,1PE13.6,' },',/))
2004  FORMAT( 3X,' {',1PE13.6,',',5X,1PE13.6,' }}')
      END
```

C-3. Ray Path Example

The following is a plot of the position of the limiting ray for the conditions used to present the data in this paper. The shadow zone is to the right of the curve minimum in the figure and between the curve and the range axis. The maximum height indicated at a range of 7000 m is 76.2 m. The shadow zone begins at a range of 1835.29 m.

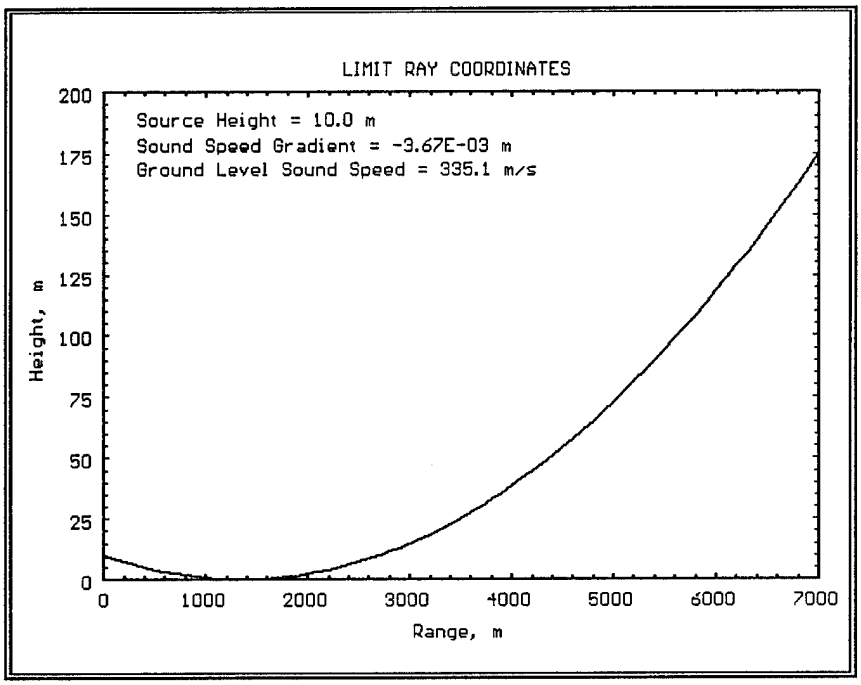

Figure C-2. Shadow zone limit ray coordinates.

Appendix D

Producing Contour Plots in Mathematica

Mathematica has an extensive graphics capability including generation of contour plots. The Mathematica book [1] gives simple commands for producing plots on the screen, while in a Mathematica session. However, the default settings for the options are not always the desirable ones. For example, axis labels are entered at the end of the axis rather than along side the axis. The best way to generate a plot is to do a simple plot command in an assignment statement (i.e., p = ListPlot[list]) and then Edit[p]). The full range of options are part of the definition of p at this point. These options may then be changed as desired. Once p is properly done, it can be preserved by Save["filename",p]. This is how the object u was preserved in the file amp5-7c2.plt recorded below. Data for u is defined to begin at (5040, 2) rather than at (0, 0). Another peculiarity of Mathematica is that under these circumstances, axis annotation at (5000, 0) is not written. Appropriate entries to correct these type of defects are included in the Epilog option. Setting the Background and DefaultColor options as shown below is important when a Word Perfect version is to be produced. Version 2.0 of Mathematica is the version employed here. Conversion of the PostScript plot file to Encapsulated PostScript (EPS) format has not yet been done successfully. The latter may be converted directly into WPG format without going through the GRAB utility when a successful PostScript conversion is achieved.

The Mathematica commands for producing the plot of figure 7 in the main text are contained in a file named AMP5-7C2.PLT which is included below.

```
(*  This is file c:\projects\acoustic\ampprept\amp5-7c2.plt which was
last modified 6 May, 1992 by Harry J. Auvermann.  This file is for
input into MATHEMATICA with the purposed of creating plots of contour
data.  The objects defined here are Lists t and s and functions w and
z.  The contour data is in the object g which is a square two index
List.  The object u actually does the contour plot.  Function z has the
option AspectRatio set to 1 to enable the graphic output region to be
defined by object t.  *)

(*  Object s draws a line very near the boundary of t to mark out the
plot region.  Function w creates a smaller rectangle placed within s
into which the contour plot is placed as indicated by the fact that the
third argument in the Rectangle call is the dummy argument x.  The
sequence is that the data is brought into g, perhaps by g =
<<amp5-7c2.dat, Edit[u] is invoked to modify u if needed, the object r
is created by r = w[u], and finally v is created by v = z[r].  The List
g is defined below with a limited number of entries to save time while
working out the details of the plot.  Once the plot details are
```

```
satisfactory, Clear[g], then Get the desired data file and run r and v
again.  The list l is intended to plot a limit ray curve.  To save the
results, the Display function is used to produce a PostScript file such
as Display["amp5-7c2.ps",v].  *)

(*  Use the GRAB utility from DRAWPERFECT to produce a file such as
amp5-7c2.wpg that is suitable for input to a WORDPERFECT document.  *)

l = ReadList["lim5-7c2.dat",{Number,Number}]

g    =    {{-129.,    -129.2493781056045,    -129.9901951359278,
-131.2015325445528,
   -132.851648071345, -134.9016994374947, -137.309518948453,
   -140.0327780786685, -143.0312423743285, -146.2681202353685,
   -149.7106781186547}, {-124., -124.2769256906871,
-125.0977222864644,
   -126.4341649025257, -128.2442890089805, -130.478150704935,
   -133.0832691319598, -136.0087712549569, -139.2079728939615,
   -142.6396103067893, -146.2681202353685},
   {-119., -119.3112887414927, -120.2310562561766,
-121.7200187265876,
   -123.7213595499958, -126.169905660283, -129.,
-132.1507290636732,
   -135.5685424949238, -139.2079728939615, -143.0312423743285},
   {-114., -114.3553390593274, -115.4005494464026,
-117.0788655293195,
   -119.3112887414927, -122.0116263352131, -125.0977222864644,
   -128.4974746830583, -132.1507290636732, -136.0087712549569,
   -140.0327780786685}, {-109., -109.4138126514911,
-110.6227766016838,
   -112.5410196624968, -115.0555127546399, -118.0512483795332,
   -121.4264068711929, -125.0977222864644, -129.,
-133.0832691319598,
   -137.309518948453}, {-104., -104.4950975679639,
-105.9258240356725,
   -108.1547594742265, -111.0156211871642, -114.3553390593274,
   -118.0512483795332, -122.0116263352131, -126.169905660283,
   -130.478150704935, -134.9016994374947},
   {-99., -99.6155281280883, -101.3606797749979, -104.,
-107.2842712474619,
   -111.0156211871642, -115.0555127546399, -119.3112887414927,
   -123.7213595499958, -128.2442890089805, -132.851648071345},
   {-94., -94.8113883008419, -97.0277563773199, -100.2132034355964,
-104.,
   -108.1547594742265, -112.5410196624968, -117.0788655293195,
   -121.7200187265876, -126.4341649025257, -131.2015325445528},
   {-89., -90.180339887499, -93.1421356237309, -97.0277563773199,
   -101.3606797749979, -105.9258240356725, -110.6227766016838,
   -115.4005494464026, -120.2310562561766, -125.0977222864644,
   -129.9901951359278}, {-84., -86.0710678118655, -90.180339887499,
   -94.8113883008419, -99.6155281280883, -104.4950975679639,
```

```
   -109.4138126514911, -114.3553390593274, -119.3112887414927,
   -124.2769256906871, -129.2493781056045},
   {-79.00000000000002, -84., -89., -94., -99., -104., -109., -114.,
-119.,
   -124., -129.}}

t = {GrayLevel[1.], Rectangle[{0., 0.}, {1., 1.}]}

s = {Thickness[0.001], Line[{{0.001, 0.001}, {0.001, 0.999}, {0.999,
0.999},
   {0.999, 0.001}, {0.001, 0.001}}]}

w[x_] := {Rectangle[{0.08, 0.08}, {0.92, 0.92}, x]}

u =ContourGraphics[g, {PlotRange -> {-80, -115},
   DisplayFunction ->
   ((Display["d:\\tempfile", #1];
      Run["msdosps -monitor 1 -device vgahi d:\\tempfile"];
      Run["del d:\\tempfile"]; #1) & ), ColorOutput -> Automatic,
   Axes -> None, AxesOrigin -> {0, 0}, PlotLabel -> None, AxesLabel
-> None,
   Ticks -> None, Frame -> True, Prolog -> {},
   Epilog -> {Text["AMPP PROGRAM CONTOURS", Scaled[{0.5, 1.05}]],
      Text["Range, m", Scaled[{0.5, -0.1}]],
      Text["Height, m", Scaled[{-0.04, 0.43}], {0, 0}, {0, 1}],
      Text["5000", Scaled[{0.005, -0.035}]],
      Text["0", Scaled[{-0.023, 0.001}]],
      {Thickness[0.004], Line[1]}, {Thickness[0.001]}}, AxesStyle
-> Automatic,
   Background -> GrayLevel[1], DefaultColor -> GrayLevel[0],
   Contours -> {-80., -85., -90., -95., -100., -105., -110., -115.},
   ContourShading -> False, ContourSmoothing -> Automatic,
   AspectRatio -> 1., MeshRange -> {{5040., 7000.}, {4., 200.}}}]

r = w[u]

z[q_] := Show[Graphics[t], Graphics[s], Graphics[q], AspectRatio -> 1]

v = z[r]
```

Distribution

	Copies
ARMY CHEMICAL SCHOOL ATZN CM CC ATTN MR BARNES FT MCCLELLAN AL 36205-5020	1
NASA MARSHAL SPACE FLT CTR ATMOSPHERIC SCIENCES DIV E501 ATTN DR FICHTL HUNTSVILLE AL 35802	1
NASA SPACE FLT CTR ATMOSPHERIC SCIENCES DIV CODE ED 41 1 HUNTSVILLE AL 35812	1
ARMY STRAT DEFNS CMND CSSD SL L ATTN DR LILLY PO BOX 1500 HUNTSVILLE AL 35807-3801	1
ARMY MISSILE CMND AMSMI RD AC AD ATTN DR PETERSON REDSTONE ARSENAL AL 35898-5242	1
ARMY MISSILE CMND AMSMI RD AS SS ATTN MR H F ANDERSON REDSTONE ARSENAL AL 35898-5253	1
ARMY MISSILE CMND AMSMI RD AS SS ATTN MR B WILLIAMS REDSTONE ARSENAL AL 35898-5253	1

ARMY MISSILE CMND 1
AMSMI RD DE SE
ATTN MR GORDON LILL JR
REDSTONE ARSENAL
AL 35898-5245

ARMY MISSILE CMND 1
REDSTONE SCI INFO CTR
AMSMI RD CS R DOC
REDSTONE ARSENAL
AL 35898-5241

ARMY MISSILE CMND 1
AMSMI
REDSTONE ARSENAL
AL 35898-5253

ARMY INTEL CTR 1
AND FT HUACHUCA
ATSI CDC C
FT HUACHUCA AZ 85613-7000

NORTHROP CORPORATION 1
ELECTR SYST DIV
ATTN MRS T BROHAUGH
2301 W 120TH ST BOX 5032
HAWTHORNE CA 90251-5032

NAVAL WEAPONS CTR 1
CODE 3331
ATTN DR SHLANTA
CHINA LAKE CA 93555

PACIFIC MISSILE TEST CTR 1
GEOPHYSICS DIV
ATTN CODE 3250
POINT MUGU CA 93042-5000

LOCKHEED MIS & SPACE CO 1
ATTN KENNETH R HARDY
ORG 91 01 B 255
3251 HANOVER STREET
PALO ALTO CA 94304-1191

NAVAL OCEAN SYST CTR
CODE 54
ATTN DR RICHTER
SAN DIEGO CA 92152-5000 1

METEOROLOGIST IN CHARGE
KWAJALEIN MISSILE RANGE
PO BOX 67
APO SAN FRANCISCO
CA 96555 1

DEPT OF COMMERCE CTR
MOUNTAIN ADMINISTRATION
SPPRT CTR LIBRARY R 51
325 S BROADWAY
BOULDER CO 80303 1

DR HANS J LIEBE
NTIA ITS S 3
325 S BROADWAY
BOULDER CO 80303 1

NCAR LIBRARY SERIALS
NATL CTR FOR ATMOS RSCH
PO BOX 3000
BOULDER CO 80307-3000 1

DEPT OF COMMERCE CTR
325 S BROADWAY
BOULDER CO 80303 1

DAMI POI
WASH DC 20310-1067 1

MIL ASST FOR ENV SCI OFC
OF THE UNDERSEC OF DEFNS
FOR RSCH & ENGR R&AT E LS
PENTAGON ROOM 3D129
WASH DC 20301-3080 1

DEAN RMD
ATTN DR GOMEZ
WASH DC 20314 1

SPACE NAVAL WARFARE
SYST CMND
PMW 145 1G
WASH DC 20362-5100 1

ARMY INFANTRY
ATSH CD CS OR
ATTN DR E DUTOIT
FT BENNING GA 30905-5090 1

AIR WEATHER SERVICE
TECH LIBRARY FL4414 3
SCOTT AFB IL 62225-5458 1

USAFETAC DNE
ATTN MR GLAUBER
SCOTT AFB IL 62225-5008 1

HQ AWS DOO 1
SCOTT AFB IL 62225-5008 1

ARMY SPACE INSTITUTE
ATTN ATZI SI 3
FT LEAVENWORTH
KS 66027-5300 1

PHILLIPS LABORATORY
PL LYP
ATTN MR CHISHOLM
HANSCOM AFB MA 01731-5000 1

ATMOSPHERIC SCI DIV
GEOPHYSICS DIRCTRT
PHILLIPS LABORATORY
HANSCOM AFB MA 01731-5000 1

PHILLIPS LABORATORY
PL LYP 3
HANSCOM AFB MA 01731-5000 1

RAYTHEON COMPANY
ATTN DR SONNENSCHEIN
528 BOSTON POST ROAD
SUDBURY MA 01776
MAIL STOP 1K9 1

ARMY MATERIEL SYST 1
ANALYSIS ACTIVITY
AMXSY
ATTN MP H COHEN
APG MD 21005-5071

ARMY MATERIEL SYST 1
ANALYSIS ACTIVITY
AMXSY AT
ATTN MR CAMPBELL
APG MD 21005-5071

ARMY MATERIEL SYST 1
ANALYSIS ACTIVITY
AMXSY CR
ATTN MR MARCHET
APG MD 21005-5071

ARL CHEMICAL BIOLOGY 1
NUC EFFECTS DIV
AMSRL SL CO
APG MD 21010-5423

ARMY MATERIEL SYST 1
ANALYSIS ACTIVITY
AMXSY
APG MD 21005-5071

NAVAL RESEARCH LABORATORY 1
CODE 4110
ATTN MR RUHNKE
WASH DC 20375-5000

ARMY MATERIEL SYST 1
ANALYSIS ACTIVITY
AMXSY CS
ATTN MR BRADLEY
APG MD 21005-5071

ARMY RESEARCH LABORATORY 1
AMSRL D
2800 POWDER MILL ROAD
ADELPHI MD 20783-1145

ARMY RESEARCH LABORATORY 1
AMSRL OP SD TP
TECHNICAL PUBLISHING
2800 POWDER MILL ROAD
ADELPHI MD 20783-1145

ARMY RESEARCH LABORATORY 1
AMSRL OP CI SD TL
2800 POWDER MILL ROAD
ADELPHI MD 20783-1145

ARMY RESEARCH LABORATORY 1
AMSRL SS SH
ATTN DR SZTANKAY
2800 POWDER MILL ROAD
ADELPHI MD 20783-1145

ARMY RESEARCH LABORATORY 1
AMSRL
2800 POWDER MILL ROAD
ADELPHI MD 20783-1145

NATIONAL SECURITY AGCY W21 1
ATTN DR LONGBOTHUM
9800 SAVAGE ROAD
FT GEORGE G MEADE
MD 20755-6000

ARMY AVIATION CTR 1
ATZQ D MA
ATTN MR HEATH
FT RUCKER AL 36362

OIC NAVSWC 1
TECH LIBRARY CODE E 232
SILVER SPRINGS
MD 20903-5000

ARMY RSRC OFC 1
ATTN DRXRO GS
PO BOX 12211
RTP NC 27009

DR JERRY DAVIS 1
NCSU
PO BOX 8208
RALEIGH NC 27650-8208

ARMY CCREL
CECRL GP
ATTN DR DETSCH
HANOVER NH 03755-1290
1

ARMY ARDEC
SMCAR IMI I BLDG 59
DOVER NJ 07806-5000
1

ARMY SATELLITE COMM AGCY
DRCPM SC 3
FT MONMOUTH NJ 07703-5303
1

ARMY COMMUNICATIONS
ELECTR CTR FOR EW RSTA
AMSEL EW D
FT MONMOUTH NJ 07703-5303
1

ARMY COMMUNICATIONS
ELECTR CTR FOR EW RSTA
AMSEL EW MD
FT MONMOUTH NJ 07703-5303
1

ARMY DUGWAY PROVING GRD
STEDP MT DA L 3
DUGWAY UT 84022-5000
1

ARMY DUGWAY PROVING GRD
STEDP MT M
ATTN MR BOWERS
DUGWAY UT 84022-5000
1

DEPT OF THE AIR FORCE
OL A 2D WEATHER SQUAD MAC
HOLLOMAN AFB
NM 88330-5000
1

PL WE
KIRTLAND AFB NM
87118-6008
1

USAF ROME LAB TECH
CORRIDOR W STE 262 RL SUL
26 ELECTR PKWY BLD 106
GRIFFISS AFB
NY 13441-4514
1

AFMC DOW 1
WRIGHT PATTERSON AFB
OH 0334-5000

ARMY FIELD ARTLLRY SCHOOL 1
ATSF TSM TA
FT SILL OK 73503-5600

NAVAL AIR DEV CTR 1
CODE 5012
ATTN AL SALIK
WARMINISTER PA 18974

ARMY FOREGN SCI TECH CTR 1
CM
220 7TH STREET NE
CHARLOTTESVILLE
VA 22901-5396

NAVAL SURFACE WEAPONS CTR 1
CODE G63
DAHLGREN VA 22448-5000

ARMY OEC 1
CSTE EFS
PARK CENTER IV
4501 FORD AVE
ALEXANDRIA VA 22302-1458

ARMY CORPS OF ENGRS 1
ENGR TOPOGRAPHICS LAB
ETL GS LB
FT BELVOIR VA 22060

TAC DOWP 1
LANGLEY AFB
VA 23665-5524

ARMY TOPO ENGR CTR 1
CETEC ZC 1
FT BELVOIR VA 22060-5546

LOGISTICS CTR 1
ATCL CE
FT LEE VA 23801-6000

SCI AND TECHNOLOGY
101 RESEARCH DRIVE
HAMPTON VA 23666-1340 1

ARMY NUCLEAR CML AGCY
MONA ZB BLDG 2073
SPRINGFIELD VA 22150-3198 1

ARMY FIELD ARTLLRY SCHOOL
ATSF F FD
FT SILL OK 73503-5600 1

USATRADOC
ATCD FA
FT MONROE VA 23651-5170 1

ARMY TRADOC ANALYSIS CTR
ATRC WSS R
WSMR NM 88002-5502 1

ARMY RESEARCH LABORATORY
AMSRL BE M
BATTLEFIELD ENVIR DIR
WSMR NM 88002-5501 1

ARMY RESEARCH LABORATORY
AMSRL BE A
BATTLEFIELD ENVIR DIR
WSMR NM 88002-5501 1

ARMY RESEARCH LABORATORY
AMSRL BE W
BATTLEFIELD ENVIR DIR
WSMR NM 88002-5501 1

ARMY RESEARCH LABORATORY
AMSRL BE
ATTN MR VEAZEY
BATTLEFIELD ENVIR DIR
WSMR NM 88002-5501 1

DEFNS TECH INFO CTR
CENTER DTIC BLS
BLDG 5 CAMERON STATION
ALEXANDRIA
VA 22304-6145 1

ARMY MISSILE CMND AMSMI REDSTONE ARSENAL AL 35898-5243	1
ARMY DUGWAY PROVING GRD STEDP 3 DUGWAY UT 84022-5000	1
USATRADOC ATCD FA FT MONROE VA 23651-5170	1
ARMY FIELD ARTLRY SCHOOL ATSF FT SILL OK 73503-5600	1
WSMR TECH LIBRARY BR STEWS IM IT WSMR NM 88001	1
Record Copy	10
Total	96